Microwave Performance Characterization of Large Space Antennas

May 15, 1977

1. Report No. JPL Pub. 77-21	2. Government Accession No.	3. Recipient's Catalog No.
4. Title and Subtitle MICROWAVE PERFORMANCE CHARACTERIZATION OF LARGE SPACE ANTENNAS		5. Report Date May 15, 1977
		6. Performing Organization Code
7. Author(s) D. A. Bathker		8. Performing Organization Report No.
9. Performing Organization Name and Address JET PROPULSION LABORATORY California Institute of Technology 4800 Oak Grove Drive Pasadena, California 91103		10. Work Unit No.
		11. Contract or Grant No. NAS 7-100
		13. Type of Report and Period Covered JPL Publication
12. Sponsoring Agency Name and Address NATIONAL AERONAUTICS AND SPACE ADMINISTRATION Washington, D.C. 20546		
		14. Sponsoring Agency Code

15. Supplementary Notes

16. Abstract

The purpose of this report is to place in perspective various broad classes of microwave antenna types and to discuss key functional and qualitative limitations. The goal is to assist the user and program manager groups in matching applications with anticipated performance capabilities of large microwave space antenna configurations with apertures generally from 100 wavelengths upwards. The microwave spectrum of interest is taken from 500 MHz to perhaps 1000 GHz. The types of antennas discussed are phased arrays, lenses, reflectors, and hybrid combinations of phased arrays with reflectors or lenses. The performance characteristics of these broad classes of antennnas are examined and compared.

Given that large antennas in space are required in the 50-dB-gain category, the passive reflector type antenna remains the only demonstrated approach, albeit the available demonstrations are using ground-based reflectors. When high-gain systems are considered in the context of low-noise-level reception, the reflector antennas class is found virtually lossless and therefore desirable; further, the reflector bandwidth is limited only by the feed used and the structural surface tolerance. For systems requiring high gain and modest scan capability, hybrid combinations of a reflector fed by a small phased array are an attractive approach. For systems requiring wide scan capability, there appears to be no substitute for a full phased array; however, no demonstrations in the above 50-dB-gain category have been reported. Within the 30-50-dB-gain antenna category, specific requirements must be carefully assessed to arrive at the best configuration.

17. Key Words (Selected by Author(s)) Spacecraft Communications, Command and Tracking Communications	18. Distribution Statement Unclassified – Unlimited

19. Security Classif. (of this report) Unclassified	20. Security Classif. (of this page) Unclassified	21. No. of Pages	22. Price

HOW TO FILL OUT THE TECHNICAL REPORT STANDARD TITLE PAGE

Make items 1, 4, 5, 9, 12, and 13 agree with the corresponding information on the report cover. Use all capital letters for title (item 4). Leave items 2, 6, and 14 blank. Complete the remaining items as follows:

3. Recipient's Catalog No. Reserved for use by report recipients.

7. Author(s). Include corresponding information from the report cover. In addition, list the affiliation of an author if it differs from that of the performing organization.

8. Performing Organization Report No. Insert if performing organization wishes to assign this number.

10. Work Unit No. Use the agency-wide code (for example, 923-50-10-06-72), which uniquely identifies the work unit under which the work was authorized. Non-NASA performing organizations will leave this blank.

11. Insert the number of the contract or grant under which the report was prepared.

15. Supplementary Notes. Enter information not included elsewhere but useful, such as: Prepared in cooperation with... Translation of (or by)... Presented at conference of... To be published in...

16. Abstract. Include a brief (not to exceed 200 words) factual summary of the most significant information contained in the report. If possible, the abstract of a classified report should be unclassified. If the report contains a significant bibliography or literature survey, mention it here.

17. Key Words. Insert terms or short phrases selected by the author that identify the principal subjects covered in the report, and that are sufficiently specific and precise to be used for cataloging.

18. Distribution Statement. Enter one of the authorized statements used to denote releasability to the public or a limitation on dissemination for reasons other than security of defense information. Authorized statements are "Unclassified—Unlimited, " "U. S. Government and Contractors only, " "U. S. Government Agencies only, " and "NASA and NASA Contractors only. "

19. Security Classification (of report). NOTE: Reports carrying a security classification will require additional markings giving security and down-grading information as specified by the Security Requirements Checklist and the DoD Industrial Security Manual (DoD 5220.22-M).

20. Security Classification (of this page). NOTE: Because this page may be used in preparing announcements, bibliographies, and data banks, it should be unclassified if possible. If a classification is required, indicate separately the classification of the title and the abstract by following these items with either "(U)" for unclassified, or "(C)" or "(S)" as applicable for classified items.

21. No. of Pages. Insert the number of pages.

22. Price. Insert the price set by the Clearinghouse for Federal Scientific and Technical Information or the Government Printing Office, if known.

Microwave Performance Characterization of Large Space Antennas

Edited by D. A. Bathker

May 15, 1977

ii

PREFACE

In the spring of 1977, under the auspices of the Director's Office, and organized by Mr. R. V. Powell, a brief but intensive Large Space Antenna Study was conducted at the Jet Propulsion Laboratory, with participation from several key in-house interest groups. A major question addressed in the study was, "What are the advantages and limitations of large apertures in space?" To answer that question, a number of applications were studied in sufficient detail to arrive at definite configuration recommendations. This report, in part, was meant to support those configuration choices, and may be found useful in other contexts as well.

The work described in this report was performed by the Telecommunications Science and Engineering Division of the Jet Propulsion Laboratory.

ACKNOWLEDGEMENT

ABSTRACT

The purpose of this report is to place in perspective various broad classes of microwave antenna types and to discuss key functional and qualitative limitations. The goal is to assist the user and program manager groups in matching applications with anticipated performance capabilities of large microwave space antenna configurations with apertures generally from 100 wavelengths upwards. The microwave spectrum of interest is taken from 500 MHz to perhaps 1000 GHz. The types of antennas discussed are phased arrays, lenses, reflectors, and hybrid combinations of phased arrays with reflectors or lenses. The performance characteristics of these broad classes of antennas are examined and compared.

Given that large antennas in space are required in the above 50-dB-gain category (perhaps as much as 80 to 90 dB), the passive reflector type antenna remains the only demonstrated approach, albeit the available demonstrations are using ground-based reflectors. When high-gain systems are considered in the context of low-noise-level reception, the reflector antenna class is found virtually lossless and therefore desirable; further, the reflector bandwidth is limited only by the feed used and the structural surface tolerance. For systems requiring high gain and modest scan capability, say ±15 beamwidths, hybrid combinations of a reflector fed by a small phased array are an attractive approach. For systems requiring wide scan capability, there appears to be no substitute for a full phased array; however, no demonstrations in the above 50-dB-gain category have been reported. Within the more modest gain antenna category, say 30-50 dB, specific requirements must be very carefully assessed to arrive at the best . configuration.

CONTENTS

Tables

SECTION I

INTRODUCTION

The continued exploration and exploitation of near and deep space will in part be realized through the use of large-aperture microwave frequency antennas located in low-to-synchronous orbits about the earth. Given the joint freedoms from earth surface gravity and the earth atmosphere, but perhaps tempered by the thermal vacuum environment, large space antennas in the microwave spectrum appear to enable missions not otherwise possible, and we obtain new and unhindered views otherwise unobtainable.

In this report, we accept the ambitious (and perhaps unwieldy) challenge of placing in perspective various broad classes of microwave antenna types, and to discuss certain performance characteristics and limitations. The microwave spectrum is taken from about 500 MHz upwards, with no real upper bound; however, to delimit what for some may be an uncomfortably wide range, let us adopt 1000 GHz (300 µm) as the upper end even though the spectrum to, say, 20 µm is accessible and of interest, once above the earth atmosphere. By way of further delimiting, neither very small omni-class probes or loops nor medium-size endfire or horn-class antennas will be discussed. The very specialized or unique antennas or systems such as synthetic-aperture techniques, arrays of large antennas, or various adaptive arrangements are not included in the discussion. Other active antennas, such as pilot beam steered arrays, are beyond the scope of this report.

Most sections in this report will consist largely of functional and qualitative descriptions; specific applications are, for the most part, avoided until the final section. Approximate (and it is hoped, nonargumentative) quantitative performance estimates are given wherever known and useful to the purpose.

Our goal is to provide the interested reader with increased understanding of the relationships among (and later, applications of) the antenna classes and types covered. We take the most interested readers to be in the user group and program manager categories; i.e., those who are not antenna specialists but who nevertheless require sound overviews and practical knowledge of the present state-of-the-art limitations, with the important ability to recognize valuable and realizable potential future payoffs. We intend specifically to assist the user groups and program managers in matching applications to appropriate space antenna configurations and, further, to identify key areas of large antenna performance limitations of relevance to applications.

A valuable perspective is obtainable for the present-day satellite communications field in general and modest-size spacecraft antennas in particular (Ref. 1-1).

SECTION II

OUTLINE

An outline of this report is given in Fig. 2-1. The four broad antenna classes—array, lens, reflector, and hybrid—are each subdivided as shown in the figure and briefly discussed. Scanning and multibeam capabilities are described. Next, the passive reflector discussion is emphasized, since passive reflectors are the only presently known means of realizing really large antennas—those significantly greater than 100 wavelengths on a side, or in diameter (say an order of magnitude and more). The types of conic sections frequently applied in reflector antennas are discussed. An appendix dealing specifically with an important reflector pair—paraboloids and spheres—and a fairly detailed comparison of their scan characteristics is included. The large reflector discussion continues with comments on the familiar Newtonian, Cassegrain, and Gregorian variants. Shaped reflector technology is discussed, and offset reflectors are addressed. Several key performance parameters of interest are presented in some detail. During the reading of this report, occasional referral to Fig. 2-1 may serve to assist the reader in following the intended report structure.

Stress is placed on the coherent wave applications of antennas (electromagnetic field summation) as opposed to incoherent wave applications (so-called photon buckets) and rectennas. Both of the latter are based on the principle of field-squared (or power) summation, and many of the remarks herein may not apply (phasing requirements, for example).
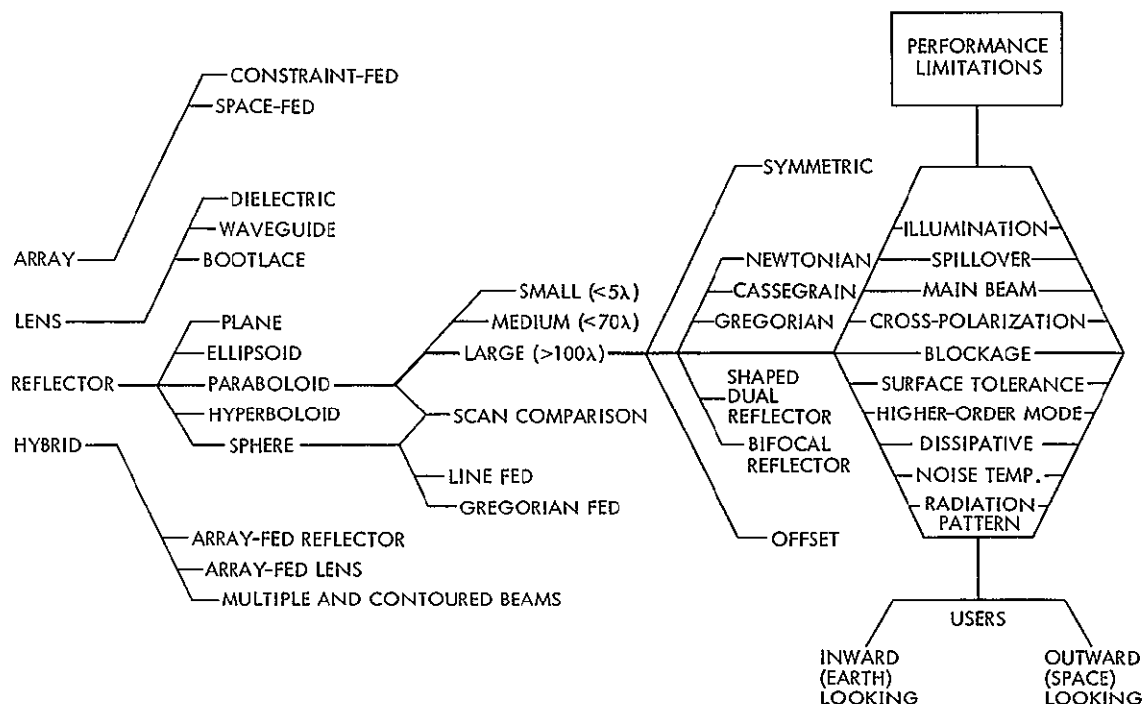
Figure 2-1. Outline: Large Antenna Characterization

We conclude with a section devoted to a cursory view of applications to aid in the selection of specific antenna types or configurations. Despite the inherent dangers in treating a broad and complex high-technology field in an abbreviated review-type manner, we believe that the goal of increasing the reader's perspective is well served by this overview document.

SECTION III

MERITS AND PRESENT PERFORMANCE OF VARIOUS ANTENNA TYPES

In this discussion, a qualitative comparison is made among antenna systems belonging to four broad classes: phased arrays, lenses, reflectors, and the so-called hybrid systems. The discussion is general and not geared to any specific application. However, maximum gain obtainable, bandwidth or bandwidth growth capability, scan or scan growth capability, and dissipation losses are the properties considered of the greatest importance.

A brief summary of the results of the following sections is given in Table 3-1. The reader is cautioned that such a table can, at best, represent only a broad generalization of performance levels; nevertheless, its value in rapidly placing the various antenna types in relative perspective perhaps overcomes its limitations.

Table 3-1. Antenna Characteristics Summary

Antenna Types	Maximum Directive Gain, dB	Minimum Beamwidth, deg	Typical Bandwidth	Typical Scan Capability	Typical Combined Losses
Phased arrays	50	0.5	±5%	±70 deg	decibels
Lenses					
Dielectric	40-45	1-2	±10%	±10 BW	decibels
Waveguide	40-45	1-2	±5%	±10 BW	decibels
Bootlace	50	0.5	±50%	±10 BW	decibels
Reflectors	~80	<0.02	Very broad; feed-limited	±4 BW[a]	Negligible
Hybrids	~70	<0.05	Broad; feed-limited	±15 BW	decibels

[a]Usual short-focus paraboloid reflector; a function of focal length to diameter ratio.

A.   PHASED ARRAYS

Phased arrays are an extraordinarly versatile class of antennas which are uniquely suitable for applications requiring beam agility. Arrays can be made conformal, that is, the elements can be flush-mounted on the surface of an aircraft or spacecraft. In many cases, conformal arrays require not only phase but also amplitude control of the element excitations. A simple solution to this problem is beyond the present state of the art. The following considerations apply mainly to the less complex planar arrays.

A broad categorization of arrays distinguishes between constraint-fed and space-fed families. To the constraint-fed category belong those arrays whose elements are excited by the radio-frequency power routed through a microwave network, which can be of the corporate or the series type. Both types of networks allow a careful control of the array illumination. The series-fed is a relatively narrowband device. Space (or optically fed) arrays may be either of the reflector type or of the lens type, resembling a reflector or a lens, respectively. The energy radiated by a feedhorn, or a cluster of feedhorns, impinges on a surface of collecting element apertures, and is reradiated from a surface of radiating elements which are connected to the collecting apertures. The advantage of optically fed phased arrays is the elimination of the hardware necessary to distribute the energy over the array aperture; on the other hand, optically fed arrays do exhibit spillover loss similar to that of lens and reflector antennas. A disadvantage is poorer illumination control, making very low sidelobes harder to obtain. Several very successful operational phased arrays are of the optically fed lens type (Ref. 3-1).

Both categories of arrays have similar and very high scan capability. With careful element design, scan angles of 60 deg from broadside can be reached with a decrease of the illumination efficiency as a function of scan angle equal almost exactly to the theoretical, that is, varying with the cosine of the scan angle. Note especially that wide scan is not a function of aperture size or beamwidth. With extra losses of 1 or 2 dB due to aperture mismatch, the scan angle can be pushed to 70 deg. Other losses are spillover (for the optical type of arrays) and feed losses such as ohmic loss in the phase shifters. Depending upon frequency, type, and number of digital phase quanta (bits) used, a loss of 1.0 dB at X-band for a ferrite 3-bit phase shifter is typical. Finally, a loss peculiar to phased arrays is the quantization loss, that is, the array gain reduction due to phase quantization. It has been shown that for an N-bit phase shifter, the mean-squared quantization error is

$$\overline{\sigma_\phi^2} = \frac{1}{12}\left(\frac{2\pi}{2^N}\right)^2$$

and the associated gain loss is equal to

$$L = 10 \log_{10} \left(1 - \overline{\sigma_\phi^2} \right)$$

For example, for N = 3,

$$L \simeq 0.3 \text{ dB}$$

Both categories of arrays tend to have practical bandwidth limitations of approximately ±5%, although it is possible to design a dual-frequency arrangement with two rather narrowband arrays of interleaved elements separated by perhaps an octave or more. Such an array would have separate corporate feeds and phase shifters for the two frequencies.

Arrays are applied in systems where beam agility is paramount (e.g., radars). Although high area efficiency is realized in some simple and modestly sized (waveguide series-fed) arrays, substantial losses are normally incurred. This detraction from overall efficiency need not map into a poorly formed beam, however; well formed and agile high-directivity beams are realized most frequently with the tradeoff of effective area as an acceptable compromise. In addition to beam agility, some phased arrays have been constructed with adaptive nulling capability, i.e., being able to steer a null of the radiation pattern to a certain direction to negate interference.

There are no obvious theoretical limitations to the gain obtainable with a phased array. Practical limitations, due to the complexity of the structure, may establish the maximum gain obtainable at the present state of the art around the value of 50 dB. Indeed, few arrays achieving this level of performance have been reported. The number of elements required exceeds ten or twenty thousand (a function of scan angle), and expenses mount rapidly. The practical limiting effects of very large numbers of elements cannot be overemphasized; nevertheless, occasional proposals for very large arrays in space are voiced.

A detailed discussion of all aspects of phased arrays is clearly beyond the scope of this report. The reader is invited to consult Refs. 3-2 and 3-3 for an extensive treatment of this subject. The preceding discussion is meant to bridge the obvious wide gap between the abbreviated presentation of Table 3-1 and the rather complete Refs. 3-2 and 3-3.

B.   LENSES

Most if not all the various types of lenses discussed share the common desirable feature of a scanning capability better than that typical of reflectors. By using a bifocal design, well formed beams can probably be obtained up to 10 beams from broadside by using simple

feeds, with an acceptable (but not high-quality) first sidelobe level of, say, -15 dB.

A possible broad classification of the various types of lenses is based on the medium of the body of the lens, namely,

(1)   dielectric (refractive index n > 1)

(2)   waveguide (refractive index n < 1)

(3)   bootlace (the refractive index concept does not apply)

Figure 3-1 shows the general configuration of a zoned waveguide lens, and Fig. 3-2 presents a bootlace lens, fed with small arrays. A brief discussion of each follows.

1.   Dielectric

The dielectric lens is the direct microwave analogy of the convergent optical lens. It is typically a very heavy and bulky structure. This drawback is partially circumvented by zoning the lens, namely by dividing its aperture into areas such that the ray paths for two different areas differ by integer multiples of a wavelength (at center frequency). Since the dielectric constant in the microwave region is independent of frequency, it is easy to realize that for frequencies different from that of design, the phase difference for two optical paths passing through two different lens zones deviates from a multiple of 360 deg. If k is the number of zones (typically three or four in modest gain applications), the bandwidth B, within which the gain loss due to the phase error introduced in the aperture illumination is not greater than approximately 1.5 dB, is

$$B = \frac{50}{k - 1}\%$$
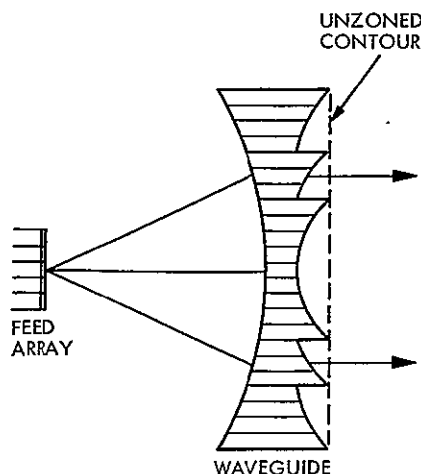
Figure 3-1.   Microwave Zoned Lens

surface located at the same distance from the lens axis. The inner face of the lens is spherical or ellipsoidal (for bifocal design). The outer face is planar (Fig. 3-2). The overall device is very broadband; the frequency limitations are due to the bandwidth of the components (radiating and collecting elements, connectors, etc.), rather than to the principle of operation. Practically, with a careful design of the radiating elements, closely spaced in terms of wavelengths at the lower-frequency band edge, a bandwidth of ±50% is possible (Ref. 3-4). The bifocal bootlace lens is capable of being scanned to wide angles (approximately ±10 beamwidths), being limited primarily by the radiating element spacing.

A practical drawback of the bootlace antenna at the present state of the art is the complexity of the structure and the delicate phase alignment of the lengths of transmission line which the lens medium consists of.

Because of the absence of zoning, a higher gain can be achieved for a bootlace lens. Although in principle, there seems to be no factor limiting the maximum gain, a practical limit of $\sim$50 dB may be dictated by structural complexity, and especially the effects of large numbers of elemental parts seen also in phased arrays.

C.   HYBRID SYSTEMS, SUMMARY

Hybrid systems, consisting of a small array of elements feeding various microwave optical systems (reflectors or lenses), form a promising class of antennas for limited scan and multibeam applications. Because of the imaging principle, the number of control elements may be drastically reduced with respect to a phased array of the same overall gain. The scanning capability may be enhanced compared to that of the associated reflector or lens, but only to a fraction of that available from a full phased array.

Considering first reflectors, the feed system array might consist of a cluster of feeds located in the focal region, fed by a network of variable power dividers. If it is desired to avoid the use of variable power dividers, a system consisting of a small lens in the focal region fed by an array focused on a point of the inner surface of the small lens can be used. A virtual feed is generated in this way, and a partial compensation of the aberration of the large reflector can be obtained. A better aberration compensation can be achieved by using, instead of the small lens, a microwave network known as a Butler matrix for a one-dimensional scan, or a system of two cascaded sets of Butler matrices for a two-dimensional scan, fed by a power divider through a set of phase shifters. A more detailed discussion is given in Appendix A. The scan capability of a one-dimensional scan Butler matrix feed reported in this appendix is ±15 beamwidths. Although data are not available, it is reasonable to assume that the maximum gain obtainable with antennas fed in this way is several decibels less than
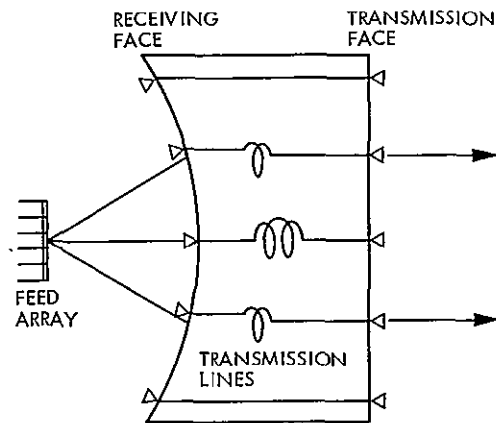
Figure 3-2. Microwave Bootlace Lens

Therefore, with zoning the modest dielectric lens is capable of reason-able bandwidth. Other sources of losses are, however, reflections at the lens faces and ohmic losses in the dielectric medium, whose combi-nation can be as high as 2 dB. Most importantly, increasing the size of the aperture requires a greater number of zones if the weight of the structure is to be kept within reasonable limits. A fundamental conse-quence of this is that the bandwidth decreases. Also a large number of zones introduces scattering at the zoning steps, with further loss of gain. A practical limit for the gain of this kind of antenna is perhaps 40 to 45 dB.

2. Waveguide

Waveguide lenses are made of a highly dispersive medium. The index of refraction is smaller than unity and decreases with frequency. Consequently, the lens profile is thicker at the edge than at the center and the bandwidth is severely limited (see Fig. 3-1). Zoning is used for this kind of lens, too, but unlike the dielectric lens, the zoning effect is that of reducing (rather than increasing) the chromatic aberration of the lens. Zoning also has the effect of reducing the variation of thickness along the lens profile, making the structure lighter. Even with zoning, the waveguide lens is an inherently narrow-band device. A typical design bandwidth for radar applications is ±2.5%. A bandwidth of ±5% can be achieved by accepting a gain loss of ∿2 dB at the edge of the band. With a long-focal-length design (to reduce the number of zones), a practical gain limit remains 40 to 45 dB.

3. Bootlace

In a bootlace lens, each collecting element on an inner lens face is connected through equal lengths of nondispersive transmission lines (coaxial cables or striplines) to a radiating element on the outer

that obtainable with the same reflector fed by a simple feed because of spillover and especially ohmic loss associated with the complex feed structure. Therefore, a gain level on the order of 70 dB should be achievable using reflectors.

Also discussed in Appendix A is another aberration compensation method using a Cassegrain antenna configuration. The normal hyperboloid subreflector is replaced by a paraboloid subreflector, and the point-source feed is replaced by a small planar phased array. This configuration seems to have scanning performance characteristics similar to that of the Butler matrix compensation method but should have less feed system dissipation loss.

For hybrid systems with a dielectric or waveguide lens substituted for the main reflector, the same feed systems as discussed for reflectors can be used. Some improvement results because of the elimination of feed blockage; on the other hand, complexity, weight, and perhaps the added dissipative loss as well must be considered. In view of the expected large dissipative losses in the feed system itself, however, the added loss due to the lens might be negligible.

When we speak of a multiple-beam antenna, we mean a single antenna generating a number of simultaneous independent pencil beams, each point-ing in a different direction. Each beam formed will thus have an inde-pendent input port for the transmit mode (or output port for the receive mode) of operation. These antennas may assume many different configura-tions, such as phased arrays, bootlace lenses, Butler arrays, as well as hybrid systems. However, there are specific characteristics that are common to all such antennas. These characteristics pertain to the beam interactions in antenna gain, patterns, and feed port isolation and are discussed in Appendix A.

An application of a multiple-beam antenna is to generate a radia-tion pattern to conform to a given geographic area as seen from geosyn-chronous orbit. For example, in Appendix A, a radiation pattern in the shape of the Eastern Time Zone of the United States has been generated.

D.   REFLECTOR ANTENNAS

1.   General Classification

The reflectors commonly used for microwave antennas are all derived from optical counterparts and generally use the conic sections for the reflecting surface. The polar form of the equation describing the conic sections is given by

$$\frac{r}{f} = \frac{1 + e}{1 + e \cos \theta}$$

, where r is distance to the surface from the origin at one pole and f is focal length; e is the eccentricity for which e = 0 describes a circle, e < 1 describes an ellipse, e = 1 describes a parabola, e > 1 is a hyperbola, and e = ∞ describes a line, as shown in Fig. 3-3. For application to antennas, the curves described are used either as conic cylinders or, more generally, reflecting surfaces generated by rotation around the focal axis to generate figures of revolution. These figures of revolution are then known as the sphere, ellipsoid, paraboloid, hyperboloid, and plane, respectively. As long as the reflectors are large (in terms of wavelengths), they are truly very broadband devices, within the obvious limits of surface tolerance effects.

Inspection of Fig. 3-3 and some thought will reveal the multiplicity of uses to which the various reflectors can be applied; that is, the focusing (converging wave) and the scattering (diverging wave) applications. As an example, consider the hyperboloid. If a spherical (diverging) wave emanating from (4, 0) is incident from the right in Fig. 3-3, the convex surface will cause the initial divergence to reverse and increase; the wave will appear to emanate from (0, 0). If, on the other hand, a planewave (no divergence) is incident from the left in Fig. 3-3 upon the concave surface of the paraboloid, the wave will converge on the focus (0, 0). Consideration of all sections (including the line or plane) will show the family of transformations possible--from planewave to planewave, to spherical wave to spherical wave of different radius or origin, and all combinations in between.
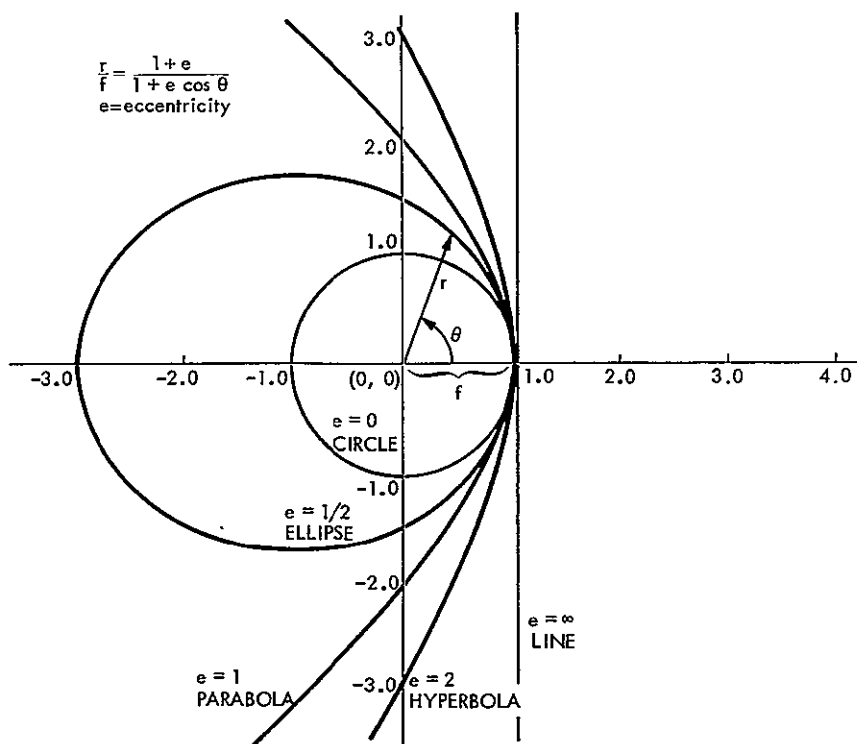
Figure 3-3. Conic Sections

Perhaps the most widely applied reflector is the paraboloid. The paraboloid has, as a key characteristic, the transforming action of a simple point-source focus to a planewave, or vice versa. This single point of spherical wave emanation (or collection) is a most valuable characteristic.

Microwave reflector antennas based on the focusing paraboloid are usually constructed as compact (short-focal-length) equivalents of the Newtonian telescope. Like the telescope, the gain or collecting area is directly proportional to aperture area, and is theoretically unlimited provided mechanical surface tolerance is maintained at the reflecting surface. The paraboloidal reflector antenna, however, when compared with phased arrays and lenses, suffers a major drawback in that beam distortion results from feed displacement from the focus of the reflector. An additional drawback is the increased sensitivity to mechanical surface deviations, compared with arrays or lenses. Because of cost, weight, and reliability factors, reflectors are generally more attractive than phased arrays or lenses. Methods of dealing with scanned beam distortion effects are given in Appendix A, and will not be addressed further here. The surface deviation effects will be discussed later.

Microwave reflector antennas based on the sphere are less common than those based on the paraboloid. For very-long-focal-length systems (e.g., optical Newtonian telescope), the deviation of a sphere from a paraboloid becomes so small as to produce a quasi-point focus. In the fully utilized short-focal-length spheres typical of large microwave structures, this is not true, and a very complex focal region must be handled or "matched" by the feed if the full area available is to be utilized. If it were not for the perfect scan capability of this conic section, the complex focus would be primarily of academic, not engineering, interest (Fig. 3-4).

There are at least two ways to match the complex focus: with a tailored line-source feed or with a rather large concave (Gregorian-type) corrector-subreflector, which transforms the complex source region to a point focus, located perhaps near the surface of the main reflector. At the point focus, relatively simple and broadband feeds (as employed in a paraboloid) are used. This system has some disadvantages: The corrector is necessarily and unavoidably large; approximately -11 dB sidelobes and somewhat reduced area and beam efficiencies result. In order to scan the system, both the feed and the corrector-subreflector must be rotated, usually implying a heavy, slow system. Nevertheless, there are applications in which such a system may prove advantageous. In the case of the line-source feed, somewhat less mass is required to be moved for scanning (Ref. 3-5). On the other hand, line-source feeds are inherently narrowband (and usually singleband) devices. Multiple-beam formation requires multiple feeds, with possible mutual physical interference. Finally, any scanned sphere must initially be under-illuminated, as stated, in order to avoid excessive spillover at the scan extremes. This, in turn, implies initial low utilization of the geometric area. Still, the length of the complex focal region is reduced when the full available area is not utilized, making the feed realization somewhat easier. This complex multiparameter problem is
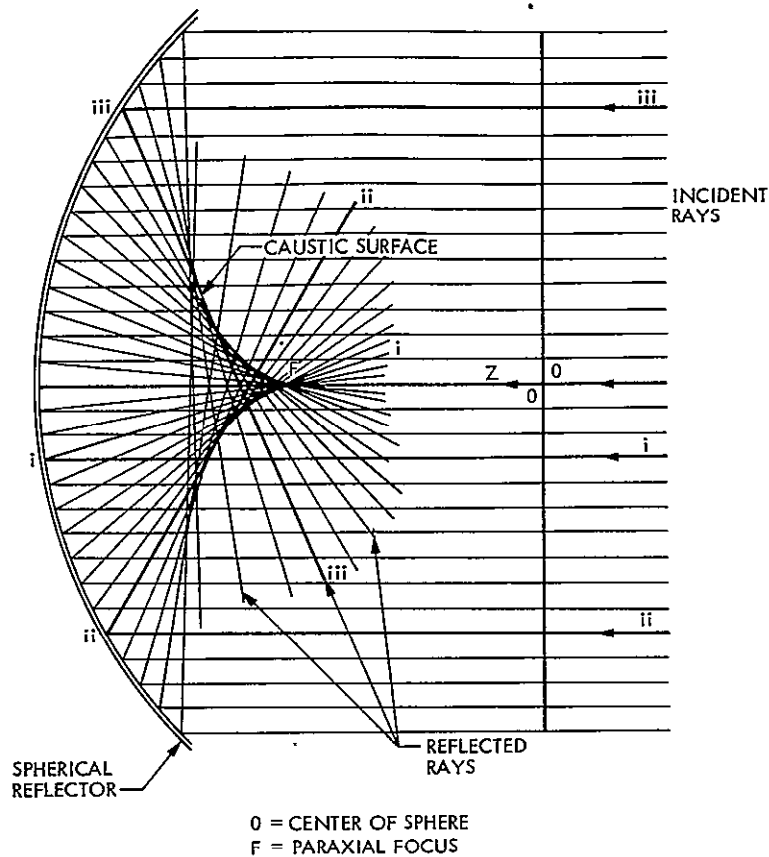
Figure 3-4. Spherical Reflector

looked at, in the context of comparison with the more conventional paraboloid, in Appendix B.

2.   Classification According to Size

In the reflector size discussions to follow, we will be generally referring to the paraboloid in its usual focusing mode, as opposed to its inverted mode, i.e., transforming a planewave to a diverging spherical wave (off the reflector "backside"). We make three reflector classifications according to size: small, medium, and large.

a.   Small Reflectors. For reflectors less than about 5 wavelengths in size (gains less than 20 dB, with halfpower beamwidths greater than 15 deg), diffraction effects dominate and rather poor overall performance is realized. Blockage, for example, tends to be severe, unless offset feeds are used. It is not generally necessary to have a precise reflector in these cases—the deviation of a corner reflector from a parabola is not great—and a corner reflector is much simpler. Usually horns or other endfire-type antennas are applied in this size regime.

b.   <u>Medium Reflectors</u>. For reflectors from 5 to about
70 wavelengths in size (gains from 20 to 45 dB, with half-power beam-
widths wider than 1 deg), the conic sections of revolution (paraboloid,
hyperboloid, ellipsoid, sphere) are frequently applied. Diffraction
effects are moderating, but still important, even for the larger sizes.
Focal point feeds are the norm since, in an axially symmetric design,
an interposed subreflector would typically be so small (say, 5 wave-
lengths) as to offer little, if any, advantage in most applications.

c.   <u>Large Reflectors</u>. For reflectors greater than 100 wave-
lengths in size (gains above 50 dB, with halfpower beamwidths less
than 0.5 deg), the paraboloid (or minor variants) is most often
applied. Ignoring relatively minor diffraction effects, the parabo-
loid bandwidth is limited by only two secondary factors: the feed
system bandwidth, which can be an octave or more without much degrada-
tion, and the surface tolerance maintained at the reflecting surface.

3.   Classification According to Configuration

For large reflectors, diffraction effects are diminishing,
allowing successful geometrical optics designs with upwards of 70%
overall aperture efficiencies. Dual and multiple reflector designs
(Cassegrain, Gregorian) are enabled on the basis of primary reflector
size, and valuable and performance-establishing design flexibilities
are therefore possible. For example, modern shaped dual-reflector
antennas have been demonstrated wherein the planewave to point-source
transformation efficiency is substantially enhanced, allowing aperture
efficiencies of over 90% (80% for the overall system), depending on
detailed definitions. More on this topic later.

Because no other antenna type has yet to achieve gains with
corresponding filled-aperture pencil beamwidths in the 70- and 80-dB
class (and more) as have paraboloids, the balance of this report will
deal primarily with this type and its variant forms. Only a few final
remarks will be made regarding scanning and multibeam capabilities.

The short-focus paraboloid reflector may be scanned only a few
beamwidths by laterally displacing the feed before the coma sidelobe
level becomes quite large, say, -13 dB. The beamwidth also broadens,
and the gain is reduced. The strongest scanning dependence is on the
f/D ratio; the larger the f/D, the farther the beam can be scanned for
the same distortions or degradations. Practical considerations have
usually limited the f/D ratio between 0.3 and 0.6 for large earth-based
structures. Space structures may enable more frequent application of
the larger f/D versions. Figure 3-5 shows beam distortions with scan
and the formation of the coma sidelobe next to the main beam in the
direction opposite of scan. In Fig. 3-5, 4 wavelengths of feed offset
correspond to 7 beamwidths of scan; the severity of both gain and
pattern degradations for this amount of scan is obvious. Figure 3-6
shows the concept of an equivalent parabola useful for comparison of
Cassegrain and Newtonian systems. In Fig. 3-6, using geometric optics
analysis, the focal length F_M of the main paraboloid is seen to be
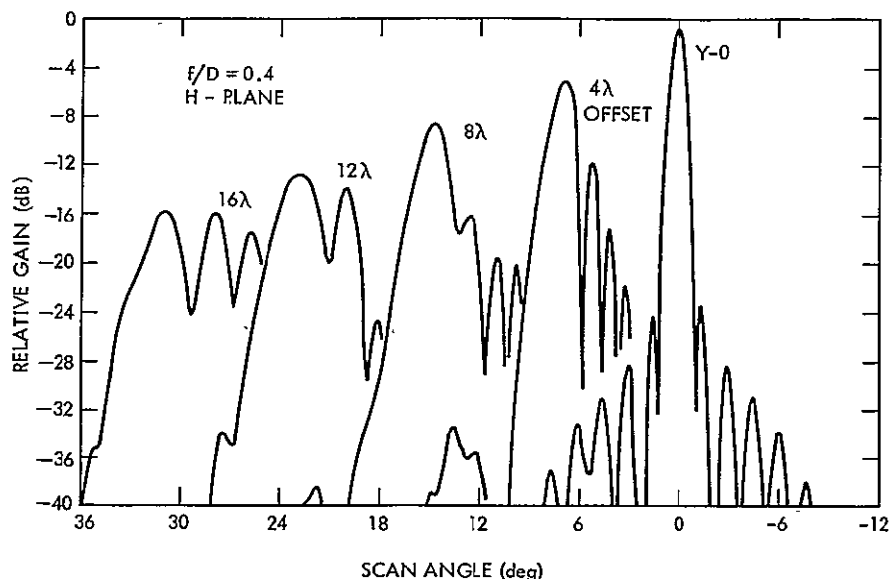
Figure 3-5. Measured Secondary Patterns as a Function
of Lateral Primary Feed Displacement

magnified to the equivalent paraboloid shown on the right-hand side,
with the much longer focal length F_c. Because of the longer effective
focal length, a simple analysis of a Cassegrain system suggests supe-
rior scanning capability. Such an oversimplified analysis does not
consider several important effects such as blockage and spillover, and
the reader is so cautioned, particularly in the context of smaller sizes.

The main disadvantage of an axially symmetric reflector as com-
pared to a lens is the gain loss and sidelobe level increase due to
feed and feed support blockage. However, this may be largely eliminated
(with complications) by using an offset reflector design. Also, as
stated, the effects of mechanical surface tolerances are more severe in
reflecting systems than in other antenna types, since a reflector
surface displacement error from the perfect surface is nearly doubled
in the optical path length due to the simple geometry of reflection.

Of the three antenna types based on the paraboloid (primary focal
point or Newtonian-fed, Cassegrain, and Gregorian), the Cassegrain is
the most frequently applied for large antennas. For the same primary
focal length, the concave (ellipsoid) Gregorian subreflector must be
larger and supported at a greater distance from the paraboloid vertex.
The advantage in doing this in some applications allows for use of the
system at extremely long wavelengths, where the subreflector has
diminished to only a few wavelengths in diameter. In this frequency
regime, the Gregorian system allows access to the prime focus for sup-
plementary direct (Newtonian-type) feeding. There are second-order
complications, however. The backlobe of the small focal-point (New-
tonian) feed is directed onto the Gregorian reflector rather than
radiating more-or less harmlessly into the front, or forward, zone of

PRINCIPAL SURFACE AND EQUIVALENT PARABOLA
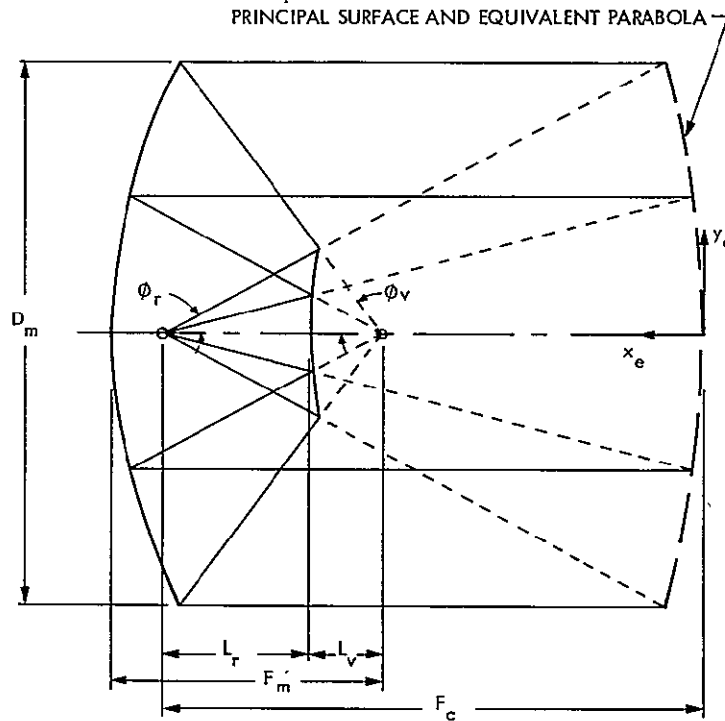
Figure 3-6. Equivalent Parabola Concept

the paraboloid, as would be the case in a pure Newtonian system. This redirected radiation shows up as alternately constructive and destructive interference, given small changes in operating frequency (chromaticity). The Cassegrain optics includes a similar (usually much smaller) effect. In each case, high-sensitivity spectroscopy measurements are hampered by this effect.

4. Shaped Dual-Reflector Antennas

A special category of axially symmetric dual-reflector antennas was developed in the mid-1960s which offers significant gain improvement over the standard paraboloid Cassegrain system (Refs. 3-6 and 3-7). This development utilized a perturbation of the hyperboloid (secondary reflector), so that the paraboloid (primary reflector) was uniformly illuminated, resulting in improved or enhanced area efficiency. (The most effective or efficient way to utilize a reflector antenna area is to illuminate it uniformly.) The paraboloid was also then perturbed as required to recover the necessary uniform phase front.

Geometrical optics is used to develop the quasi-paraboloidal surface, and so optimum operation is at infinite frequency. Studies have shown that the geometric optics synthesis is very good down to 1000 wavelengths for the quasi-paraboloid diameter. This is proven by determining the surface solutions using geometric optics and then obtaining final illumination and spillover efficiency at a specific operating frequency by using the rigors and accuracy of physical optics

theory. For the cases of apertures of 1000 wavelengths and larger, theoretical efficiencies of 98% are indicated, which include the final illumination efficiency, the forward spillover, and the back spillover. Well designed, large Cassegrain systems using hybrid-mode corrugated horns have theoretical efficiencies of 75 to 80%, which include the same items (i.e., illumination, forward and back spillover). The other contributors to efficiency reduction are essentially common to each system, i.e., phase illumination error, blockage, surface tolerance, and cross-polarization. Therefore, when using a shaped system for high efficiency or maximum gain, one can expect up to 1 dB improvement over a similar system used as a pure Cassegrain.

For the smaller systems (D ≈ 250 λ), full improvement is not available using the geometric optics synthesis, but values over 90% are realized. Diffraction synthesis techniques are still available which will maintain efficiencies of approximately 90% (meaning gain improvements on the order of 0.5 dB) down to perhaps 100 λ. Figure 3-7

*EXCLUSIVE OF
 • SURFACE TOLERANCE LOSS
 • SPAR BLOCKAGE LOSS
 • DISSIPATIVE LOSS

A) PARABOLOID – HYPERBOLOID
B) SHAPED SUB., PARABOLOID PRIMARY
C) OPTICAL SHAPED DUAL REFLECTOR
D) DIFFRACTION-SHAPED DUAL REFLECTOR
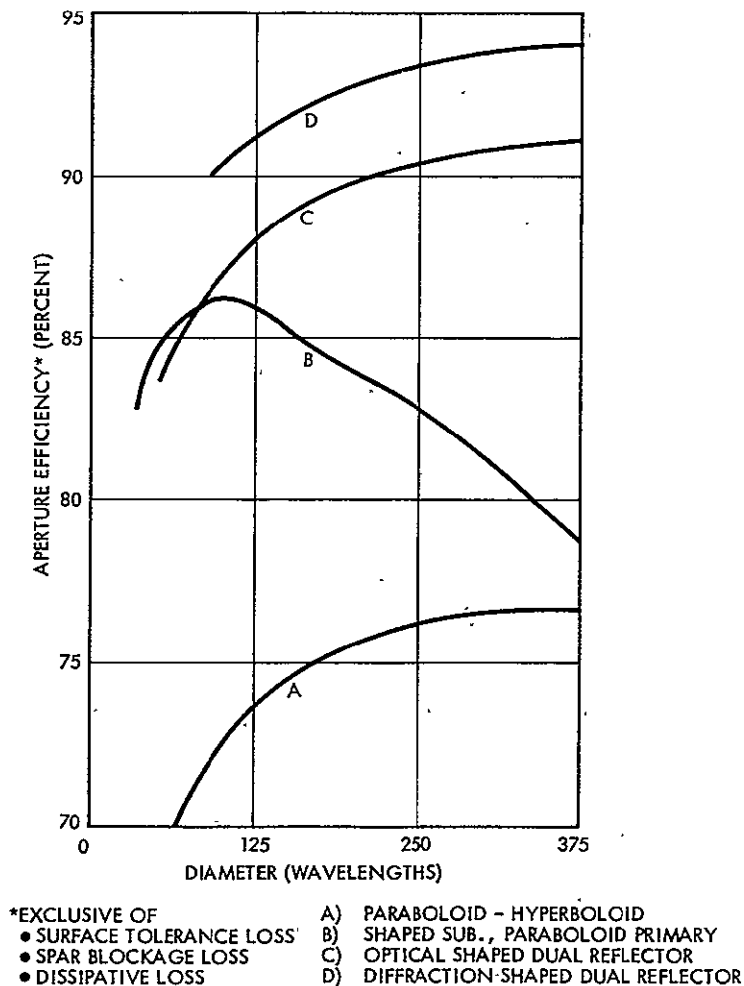
Figure 3-7. Aperture Efficiency: Dual-
Reflector Antennas

summarizes this discussion. It should be mentioned, however, that in the smaller diffraction optimized designs, bandwidth is sacrificed.

An example of typical short-focus shaped dual-reflector contours used to obtain a uniform illumination-maximum gain design is given in Fig. 3-8. Both the main and subreflectors are shown, and the design is primarily a function of the selected feedhorn taper at the edge of the subreflector, which is -23 dB in this example (a very low forward spillover design). Figure 3-9 expands the scale ten times and compares the shaped subreflector with an optical hyperboloid. In this example, the maximum axial deviation of the shaped subreflector from the hyperboloid is about 3% of the main reflector diameter, and the main reflector departs from a paraboloid by only 0.3%. In the latter case, at least, best-fitting could reduce the peak deviation by perhaps an order of magnitude.

It is now emphasized that all of the previous shaping work has been aimed at improving the illumination efficiency of reflector antennas by obtaining uniformly illuminated apertures. This results in maximum antenna gain or directivity, and also in the classical radiation pattern of the uniform circular aperture. The pattern is of the well known Bessel Function, $[J_1(x)]/x$, type, which has first sidelobes that are down by -17.6 dB. This results in a rather poor far-field main beam efficiency for many applications—about 83.8%. However, the same technique that was used to obtain uniform illumination for maximum gain may be applied to obtain a highly tapered or gaussian distribution for somewhat less gain but an extremely high beam efficiency. In this case, the blockage of the center reflector in symmetric designs would assume major importance and might be the primary contributor to any sidelobes.

The possibility of extending shaped dual-reflector antenna techniques to offset or asymmetric clear-aperture systems is discussed in Section III-5. This is expected to lead to very low sidelobe and extremely high beam efficiency designs.

5.   General Characteristics of Offset Reflectors

Although larger antennas are most commonly constructed as symmetric reflector systems, smaller offset reflector systems are now invariably employed in communication systems aboard commercial satellites. For a given aperture size, an offset clear-aperture reflector design has advantages in higher (unblocked) aperture efficiency, higher beam efficiency, and lower overall interference susceptibility. On the other hand, the offset reflector generally suffers from having more severe depolarization effects (as a result of the asymmetries) which are often hard to predict. The depolarization effects usually include a high cross-polarization level for linearly polarized systems and a beam squint (slightly nonaxial pointing) for each of the two circularly polarized waves, if used (Ref. 3-8). The comparative cost factor might also be examined prior to selection, on a common aperture size basis, since it is the projected area of the offset aperture that determines the gain. Again, the details of each application will determine the
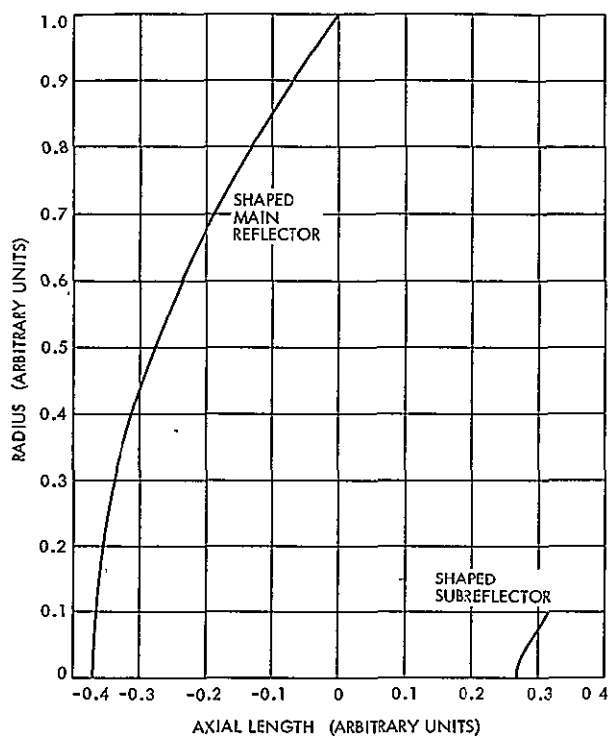
Figure 3-8. Shaped Dual Reflector: Maximum Gain Design
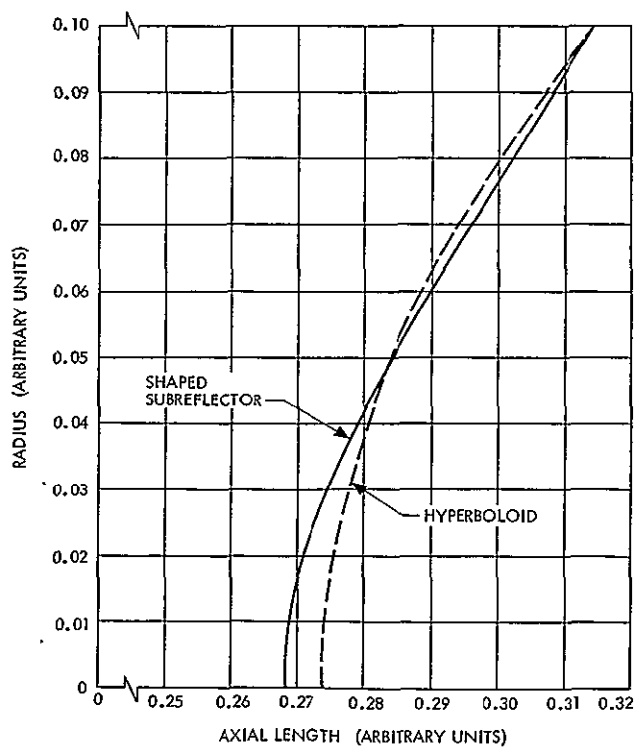
Figure 3-9. Shaped Subreflector: Maximum Gain Design

selection. Figure 3-10 shows the general layout of offset-fed single- and dual-reflector antennas, fed by small arrays.

In the past, it has not been obvious that the offset or asymmetrical paraboloid-hyperboloid system was subject to a dual-reflector antenna shaping solution. However, such a solution would be ideal for both the high area efficiency and high beam efficiency problems, since all blockage could be removed and a nearly perfect illumination function generated, tailored for each application. Just recently at JPL, in theoretical studies, it appears that a solution to this problem may indeed be possible. The solution is still being formulated, and work has just begun, but an end result may be an aperture with any selected illumination function and with no blockage whatever (Ref. 3-9).

6. Bifocal Reflectors

It is well known that a shaped dual-reflector antenna with a single focus can be used to control phase and amplitude in the main reflector aperture (Ref. 3-6). In this case, the reflectors have profiles different from the paraboloid-hyperboloid shapes. If control of amplitude is sacrificed, the phase can be controlled with a second reflector, so that an approximate bifocal dual reflector is possible (Fig. 3-11). By definition, a bifocal design would have two optically perfect focal points generating two pencil beams, each pointing in opposite off-axis directions (Refs. 3-10 and 3-11). Since highest gain is at the angles $\pm\theta_f$, the bifocal antenna has some advantage over the single-focus antenna for multiple-beam and contoured-beam applications, where the off-axis antenna gain must be maintained. However, the general approach to designing a bifocal reflector antenna leads to a double-reflector design with a ring of approximate focal points. The approximate nature of the existing design procedures sets a definite limit on how far the advantages of the bifocal reflector can be exploited. Sufficiently well documented results are not available for this relatively new reflector design, but initial results indicate that, for given specifications of gain, etc., it may be possible to double the useful range of scan obtainable with single-focus reflectors. Finally, Fig. 3-12 shows the concept of a bifocal offset dual reflector made possible by a new type of antenna reflector synthesis developed at JPL (Ref. 3-12). This concept effectively eliminates blockage effects for sidelobe and beam efficiency.

The balance of this report will deal with the conventional symmetric reflector systems, since an understanding of these systems is a foundation for a general understanding of the more complex configurations.

a) OFFSET SINGLE REFLECTOR   b) OFFSET DUAL REFLECTOR

OFFSET
PARABOLA

DISTORTED
APERTURE
DISTRIBUTION

r_2

r_1

FEED
ARRAY

MAIN
REFLECTOR

SUBREFLECTOR

FEED
ARRAY
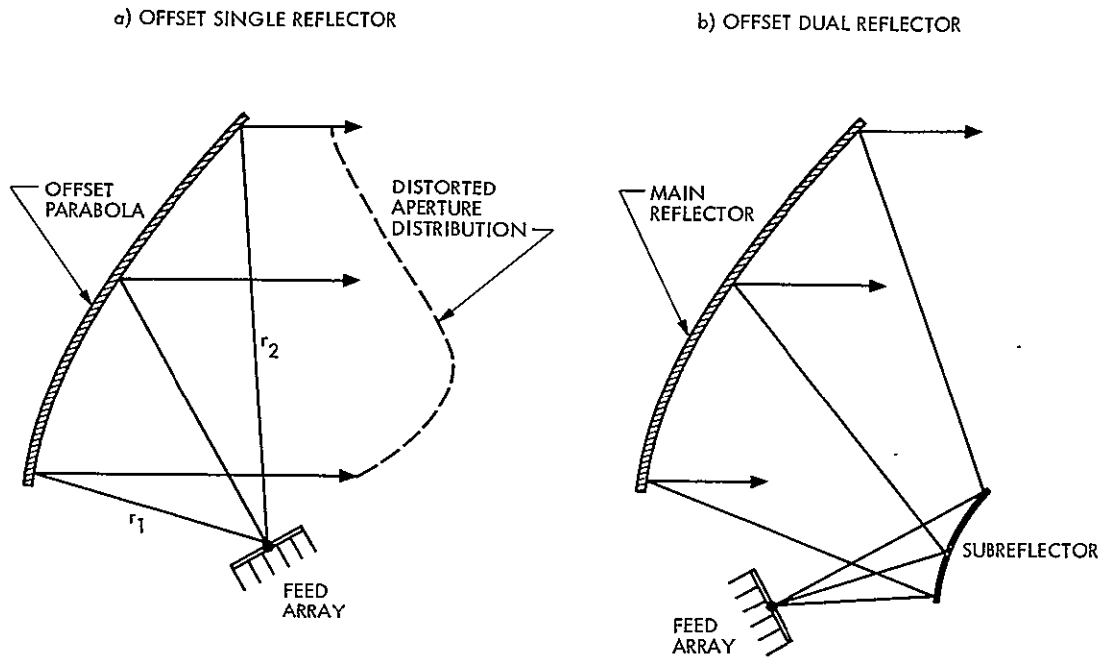
Figure 3-10.   Offset-Fed Reflectors

BEAM 1

$+\theta_f$

$-\theta_f$

BEAM 2

SHAPED
REFLECTOR

FOCUS
2

SHAPED
SUBREFLECTOR

FOCUS
1

BEAM 1

$+\theta_f$

$-\theta_f$

BEAM 2
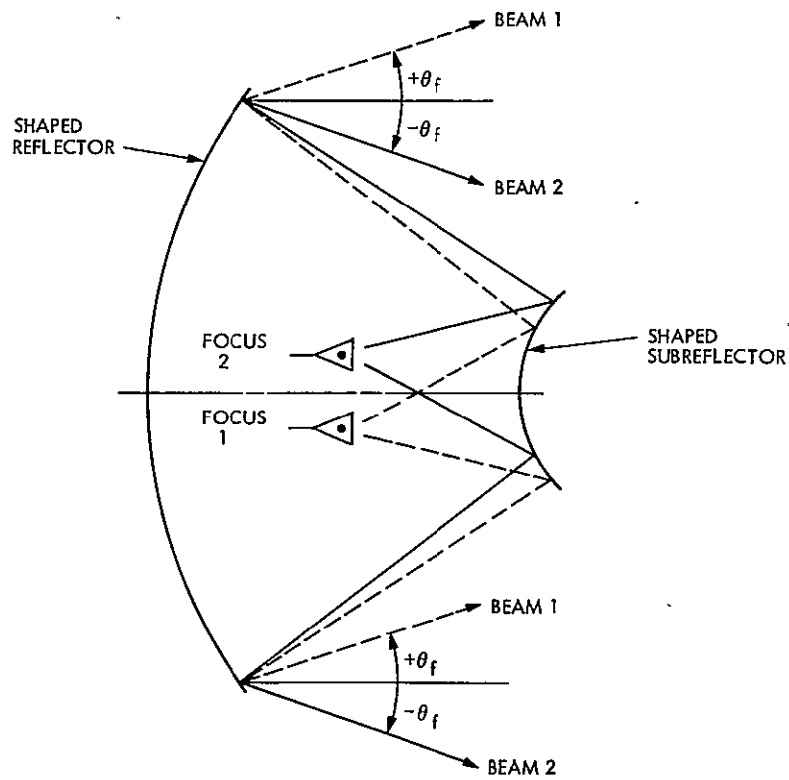
Figure 3-11.   Bifocal Dual Reflector
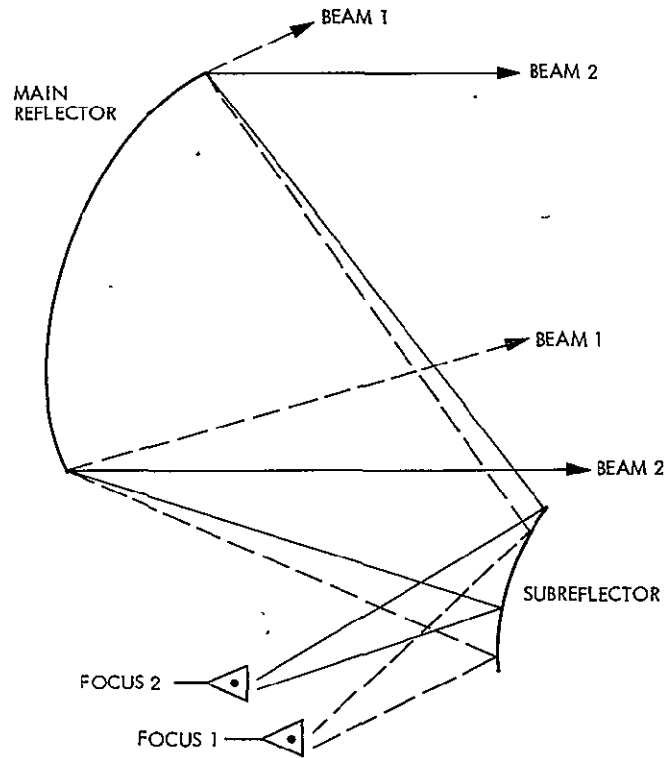
Figure 3-12. Bifocal Offset Dual Reflector

SECTION IV

KEY PERFORMANCE PARAMETERS

The microwave gain/beamwidth, main beam efficiency, and noise temperature are perhaps the most important parameters of a large single pencil-beam antenna. The gain of an aperture antenna is proportional to the collecting area projected on a plane perpendicular to the boresight of the main beam, while the beamwidth is inversely proportional to the width of the projected area. The percentage of area that is effectively used to capture the energy from an incoming planewave and coherently deliver it to the antenna input terminals is defined as the overall antenna efficiency (n_T). The gain (G) is given by

$$G = \frac{n_T 4\pi A}{\lambda^2}$$

where

G = (numeric) gain

n_T = overall antenna efficiency

λ = wavelength

A = geometric projected area

For a circular aperture, it follows that

$$G = n_T \left(\frac{\pi D}{\lambda}\right)^2 .$$

where D is the diameter of the projected area of the antenna. For the reflector-type antennas to be discussed here, the total efficiency can be expressed (and is generally analyzed) as

$$n_T = n_I n_{SP} n_X n_{BL} n_S n_M n_D$$

where

n_I = aperture illumination efficiency, including phase effects

n_{SP} = (1 - spillover loss), forward and rearward

η_X = (1 - cross-polarization loss)

η_{BL} = (1 - aperture blockage loss)

η_S = surface efficiency

η_M = (1 - higher order mode loss)

η_D = dissipative and/or reflector leakage efficiencies

As an illustrative example to set the stage for later discussion of each performance parameter, we begin by showing quantitative results of a rigorous (physical optics) analysis (of a geometric optics synthesis) of a rather modest size short-focus, shaped dual-reflector antenna of 500 wavelengths diameter (about 63 dB gain). The halfpower beamwidth of the resultant far-field beam in this illustrative example would be approximately 0.1 deg, and the far-field beam efficiency would be quite poor, say, 70-75%, since this is a heavily blocked uniform illumination (earth station) design. Table 4-1 gives the values.

For this example, certain items deserve special comment before proceeding with a full discussion of each. The blockage due to the subreflector (3% loss) is apportioned as 1% area and 2% power lost (due to slightly higher axial illumination). The blockage due to feed support (spars) (12.5% loss) is apportioned as 6.25% area and 6.25% power lost. This is typical of heavy ground antennas in the 1-g field and would be reduced to perhaps 2%, or less (for area alone) for a space antenna. Thus, the shaped, uniformly illuminated space antenna would yield an overall efficiency of 85%, all else remaining equal. A rather good reflector surface tolerance is assumed, which may not be typical of a space antenna. Finally, the assumption of zero dissipative and reflector leakage losses is also perhaps atypical of a practical space antenna.

With this as background, we will next explain and examine in an overview context each efficiency component for typical values and limits wherever possible.

A.   APERTURE ILLUMINATION EFFICIENCY

The aperture illumination (taper) efficiency (η_I) is a measure of the effectiveness of the feed to accept, or match (in reception), the uniformly distributed incident energy. Alternately, for a uniform aperture distribution, all areas of the aperture receive equal power density from the feed system (in transmission), which causes maximum utilization of the aperture and hence 100% illumination efficiency. For simple reflector-type antennas (and this applies as well to lenses and space-fed phased arrays), the radiated energy from the feed system is generally not uniform. The feed radiation is usually tapered from a maximum near the center of the aperture to a reduced intensity at the edge of -10 to -20 dB and is not zero outside the reflector region.

Table 4-1. Aperture Efficiency Evaluation, 500 λ Shaped Dual-
Reflector Antenna, Maximum Gain Design

Item	Associated Efficiency
η_I; aperture illumination efficiency	
Nonuniform amplitude	0.962
Nonuniform phase	0.983
η_{SP}; spillover efficiency	
Forward	0.990
Rear	0.997
η_X; cross-polarization	0.998
η_{BL}; blockage	
Subreflector	0.970
Spars	0.875[a]
η_S; reflector surface tolerance ($\varepsilon/\lambda = 0.01$)	0.980[a]
η_M; higher-order mode efficiency	1.000
η_D; efficiency due to dissipation/reflector leakage	1.000[a]
η_T; overall aperture efficiency	0.775

[a]Typical of earth station design.

With the present-day state of the art, simple optical Cassegrain feed
systems for large paraboloid reflectors have illumination efficiencies
of approximately 84%. This includes both amplitude and phase effects.
As was seen in the example, the efficiency is increased to about 94%
(for the two components) for the shaped dual-reflector case, and
potentially may be increased to 98%.

For a circular-aperture illumination function which tapers to
zero at the edge (so-called parabolic function), the illumination
efficiency is moderated to 75%; this would be typical of a design
requiring high far-field main beam efficiency.

B.   SPILLOVER EFFICIENCY

In the consideration of uniform aperture distribution, it was assumed that the illumination was constant at points inside the aperture and zero at points outside the aperture. This is unrealizable in an optical feed system and is analogous to a perfectly uniform filter response. In the practical case, there is energy from the feed system that radiates in directions other than that required to illuminate the aperture. The energy that falls outside the aperture is not available for collimation and is considered spillover. Since spillover is lost power, the spillover efficiency is

$$\eta_{SP} = (1 - \text{spillover})$$

Reducing the edge illumination by tapering the aperture illumination decreases spillover power and reduces sidelobes but simultaneously decreases the gain and widens the main beam. This is the primary trade-off with very small (in wavelengths) designs. Simple (optical) state-of-the-art Cassegrain feed systems for large paraboloid reflectors have forward spillover efficiencies of approximately 90-95% (still a function of gain/spillover tradeoff) and rear spillover efficiencies tailored for the application; typically 99%. As was seen in the example, these efficiencies are increased to about 99.0 and 99.7% (for the two components) for the shaped dual-reflector case.

For a circular-aperture illumination function which is caused to approach zero at each reflector edge (so-called parabolic function), the spillover efficiency would naturally approach 100%. This might come close to being realized for specially shaped reflector systems, as discussed in Section III-D4, and would be of great value in designs requiring high far-field main beam efficiency.

C.   FAR-FIELD MAIN BEAM EFFICIENCY

At this point, we temporarily interrupt the sequence of the items in Table 4-1 in order to treat the recurring topic of far-field main beam efficiency, especially because of its close relationship to spillover efficiency described in Section IV-B. It is believed that this is not a digression but rather a unifying approach to the entire topic. The far-field main beamwidth (such as the half-power beamwidth or sometimes the width between first nulls) is a common way to specify a pencil-beam antenna. Another useful way to specify antenna patterns is in terms of antenna pattern solid angle (Ref. 4-1):

$$\Omega_A = \int_0^{2\pi} \int_0^{\pi} P_n(\theta, \phi) \sin \theta d\theta d\phi$$

where Ω_A = beam solid angle, rad^2, and $P_n(\theta,\phi)$ is the normalized antenna power pattern. The beam solid angle is that solid angle through which all the power radiated from a transmitting antenna would flow if the power per unit solid angle were constant over this angle and equal to the maximum value.

If the integration is carried out only over the main lobe bounded by the first minimum instead of over the entire solid angle 4π, then the main beam solid angle is obtained by

$$\Omega_M = \iint_{\text{(MAIN LOBE)}} P_n(\theta,\phi) \sin\theta d\theta d\phi$$

where Ω_M = main beam solid angle, rad^2. The minor lobe solid angle Ω_S is defined as the residual between the beam solid angle and the main beam solid angle. Therefore,

$$\Omega_S = \Omega_A - \Omega_M$$

The far-field main beam efficiency is then defined as

$$n_B \equiv \frac{\Omega_M}{\Omega_A}$$

If the antenna is being used in the receiving mode to measure noise, n_B is the percentage of all power received which enters the main beam, assuming the antenna is surrounded by an extensive source of uniform temperature (Ref. 4-2). The main beam (or lobe) solid angle Ω_M for a uniformly illuminated circular aperture is

$$1.008 (\theta_H)^2$$

where θ_H is the half-power beamwidth, which is equal to $1.028\lambda/D$, where λ is the wavelength, and where D is the diameter of the aperture (Ref. 4-3). Therefore, in terms of λ and D, the main beam solid angle becomes

$$\Omega_M = \frac{1.065\lambda^2}{D^2}$$

Since $\Omega_A = 4\pi/D_M$, where D_M is the maximum directivity and is defined as the directivity obtainable from an antenna (assumed to be large) when the illumination is uniform over the aperture, we can express the far-field main beam efficiency as

$$\eta_B \equiv \frac{\Omega_M}{\Omega_A} = \frac{\Omega_M D_M}{4\pi} = \frac{\Omega_M}{4\pi}\left(\frac{\pi D}{\lambda}\right)^2$$

Upon substitution, the far-field main beam efficiency of a uniformly illuminated circular aperture becomes the familiar

$$\eta_B = \left(\frac{1.065\lambda^2}{D^2}\right)\left(\frac{1}{4\pi}\right)\left(\frac{\pi D}{\lambda}\right)^2 = 0.838$$

For a circular aperture with a parabolic taper, the main beam solid angle is

$$\Omega_M = 0.772(\theta_H)^2$$

where $\theta_H = 1.273\lambda/D$, becoming in terms of λ and D,

$$\Omega_M = \frac{1.251\lambda^2}{D^2}$$

and resulting in a far-field main beam efficiency of

$$\eta_B = \frac{1.251\pi}{4} = 0.983$$

Thus, maximum beam efficiency occurs for a highly tapered aperture distribution, but the maximum aperture (or area) efficiency occurs for a uniform aperture distribution. Frequently a compromise between these two extremes is used, so that a tradeoff can be made between beam and aperture efficiencies for any particular application.

The far-field main beam efficiency of a paraboloidal reflector is (strictly speaking) dependent on both the reflector illumination and the spillover efficiency factors. This is easy to realize when one

considers the spillover(s) to be added to the normal sidelobes, which are a function of illumination function. The spillover efficiency factor discussed in Section IV-B is described by (Ref. 4-4)

$$\eta_{SP} = \frac{\displaystyle\int_{\Omega'} P_F(\theta',\phi') \sin \theta' d\theta' d\phi'}{\displaystyle\int_{4\pi} P_F(\theta',\phi') \sin \theta' d\theta' d\phi'}$$

where

η_{SP} = spillover efficiency

$P_F(\theta',\phi')$ = power pattern of feed

Ω' = solid angle subtended by the reflector

In general, then, the overall far-field beam efficiency for the reflector system (assuming no blockage, surface tolerance scattering, or leakage through the surface) is the product of the two beam efficiencies.

$$\eta'_B = \eta_B \eta_{SP}$$

The high-efficiency corrugated feedhorns commonly used with Cassegrain systems have extremely low side- and backlobe radiation, and with edge illumination of the subreflector approximately 15 dB down from the feed pattern peak, the feedhorn spillover efficiency factor can be above 90 to 95%, as previously seen.

Figure 4-1 is a plot of the far-field main beam efficiency η_B as a function of rms surface tolerance for a uniformly illuminated circular aperture with the limiting case (assumed) of no central (feed) nor spar blockage. Also shown is a typical symmetric space antenna with a central blocking diameter ratio of 0.1 and moderate spar blocking with an area ratio of 0.03. Another limiting case shown is a typical ground antenna (gravity design) with a large spar blocking area ratio of 0.06. Figure 4-2 is a similar plot using a parabolic tapered aperture illumination to give an approximate upper limit to the beam efficiency obtainable from an axially symmetric reflector antenna. It can be seen that it is extremely difficult to achieve >90% far-field main beam efficiency for any symmetric reflector antenna, and the severe degradations caused by reflector surface tolerance (scattering energy out of the main beam into the minor lobe regions) are obvious. About the best far-field main beam efficiency to be expected for parabolic
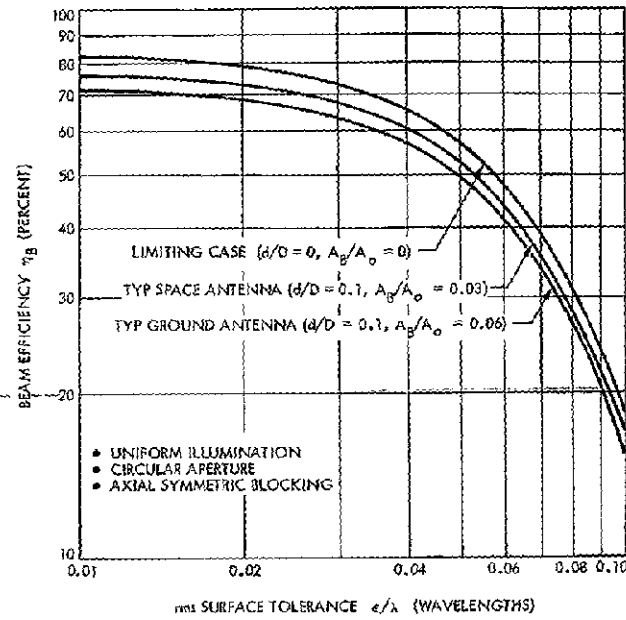
Figure 4-1.   rms Surface Tolerance Effects on Beam
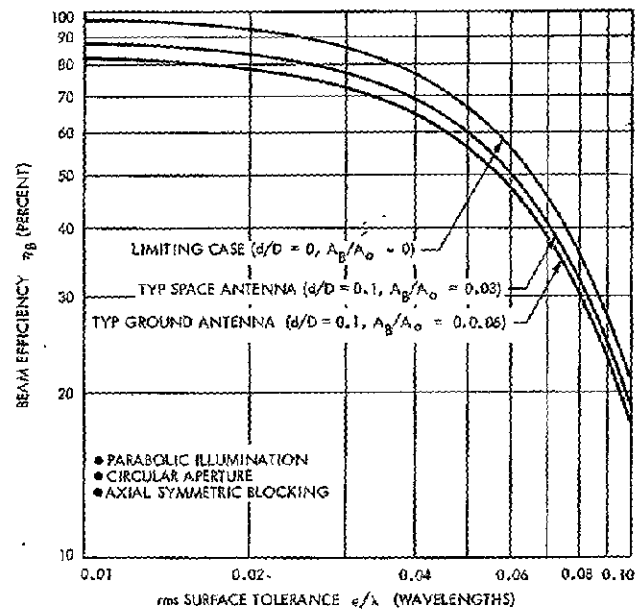Efficiency--Uniform Illumination

Figure 4-2.   rms Surface Tolerance Effects on Beam
Efficiency--Parabolic Illumination

illumination of a symmetric reflector space-class antenna is thus seen to be perhaps 85%, and that requires a very high surface precision of about 1/50 wavelength.

D.   CROSS-POLARIZATION

With present-day highly symmetric antenna feed radiation patterns such as are produced by hybrid-mode (corrugated waveguide) techniques, symmetric reflector antenna cross-polarization in general (and diagonal plane cross-polarization in particular), which formerly was a serious problem, is no longer an important consideration for the system designer (any more than the general sidelobe problem). The cross-polarization level of corrugated feeds is between -30 and -40 dB when used in a typical symmetric Cassegrain system or a Newtonian system of equivalent focal length to diameter ratio (Ref. 4-5). The polarization performance of deep paraboloids tends to be a little worse primarily because practical feeds for these reflectors generally have higher cross-polarized radiation levels. Other depolarization mechanisms in a reflector system include edge effects, surface curvature effects, and radiation from feed, subreflector, and support (spar) structures. For large paraboloids and Cassegrain systems, these effects are at least an order of magnitude less important than the purity of the feed polarization alone. From these observations, it appears that the typical cross-polarization level of present-day reflector systems is approximately -40 dB, and the corresponding efficiency term due to cross-polarization loss is very high--generally greater than 99%.

The cross-polarization lobes of an antenna act to receive cross-polarized energy (interference, noise, or general crosstalk) just as the sidelobes of an antenna receive copolarized energy. In frequency reuse space-to-ground communication systems, which utilize two orthogonal polarizations to provide two cofrequency communication channels, the cross-polarization level of the space antenna system is a primary consideration from the interference point of view. The cross-polarization level for present-day commercial satellite systems is far worse than the -40 dB quoted above and is typically in the -24 to -27 dB range (Ref. 4-6). The relatively poor polarization performance in these frequency reuse systems results from a combination of factors, including use of offset rather than symmetric reflectors, small smooth-wall horn feeds rather than corrugated horns, and a fairly broad field of view ($\pm$3 to 4 beamwidths).

An open question related to probable future implementation of really large offset reflectors, whether optical or shaped surface designs, is their resultant polarization performance. Recent work by Jacobsen has shown theoretically that copolar and cross-polar components of the radiation from a feed system are collimated separately by focused paraboloid reflectors, even for offset and for elliptical beam antennas (Ref. 4-7). The consequence of separability is that with a clean feed system, the cross-polarization of a paraboloid reflector antenna system may be removed. Experimental verification has yet to be done.

E.   HIGHER-ORDER MODE LOSSES

Many reflector systems have intentional asymmetries in their geometries. One example previously discussed is the clear-aperture system with an offset main reflector. Another example is a symmetric reflector system with an asymmetric feed arrangement, such as the NASA-JPL 64-m ground antenna shown in Fig. 4-3.

Asymmetries in the reflector or feed geometry cause the excitation of higher-order illumination pattern Fourier components with a corresponding loss of the antenna axial gain (Ref. 4-8). The field lines of different modes are shown in Fig. 4-4. Only the two $m = 1$ components contribute to radiation along the antenna axis (axial gain). The energy in the $m \neq 1$ components is radiated into unwanted directions, and thus represents a loss and a possible source of noise in the receive mode. Energy in the $m \neq 1$ components is also closely related to the depolarization characteristics of the antenna, such as the beam squint phenomenon mentioned earlier. At present, it is not clear whether these effects will become worse if more radical offsets are brought into the reflector geometry; for the case shown in Fig. 4-3, the loss of axial gain is only 2%, with corresponding increase in side radiation.

F.   APERTURE BLOCKING EFFICIENCY

A center-fed antenna, that is, one wherein the primary feed is on the symmetric axis of the main reflector, has the disadvantage of producing blocking of the aperture distribution since it is obviously in the optical path of the reflected rays. Blocking has the effect of increasing sidelobes, decreasing gain, and reducing the main beam solid angle. The decrease in gain is usually not of great importance for most large antennas, where the feed area is a small fraction of the reflector area; however, the increase in sidelobe level (and corresponding reduction in far-field beam efficiency) may be significant. The first sidelobe level with central aperture blockage may be calculated to a good approximation as follows: First calculate the far-field pattern from a knowledge of the feed characteristics and the resulting aperture illumination. This gives the normalized sidelobe level without feedhorn blocking. Now add to the normalized value twice the ratio of the central blockage area to the total aperture area. This sum is approximately the normalized sidelobe level with feed blocking. As an example, a circular aperture with a parabolic illumination has a maximum normalized sidelobe voltage level of 0.059 (-24.6 dB). A blocking area ratio of 0.02 will exhibit an approximate voltage level with feedhorn blocking of 0.059 + (2)(0.02) = 0.099 (or -20.1 dB).

Blocking also has an effect on the axial gain. If the main aperture is circular, and is assumed to have a completely tapered parabolic illumination, a small, centrally located circular blockage
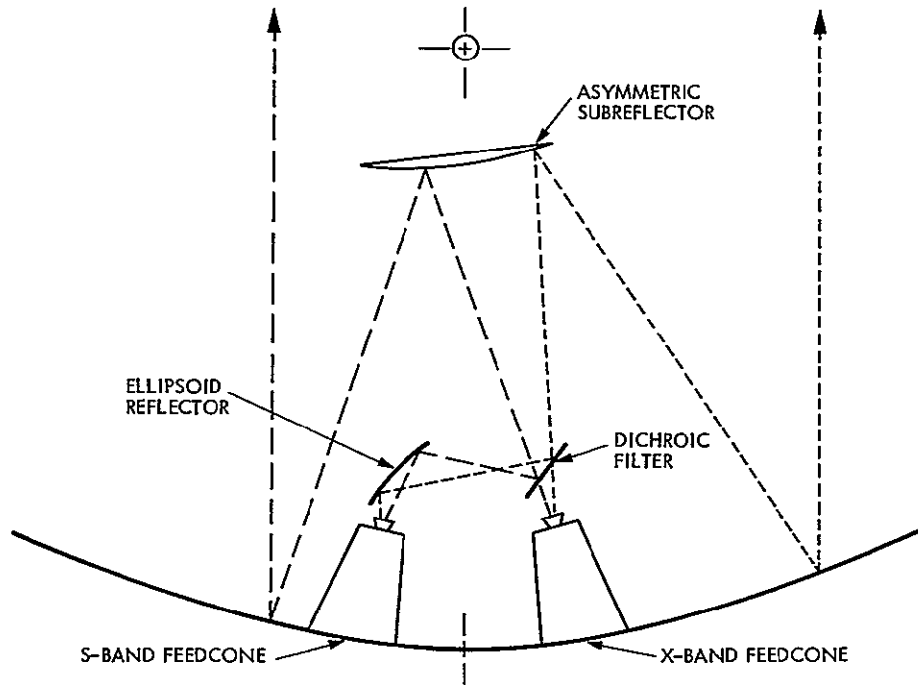
Figure 4-3. Reflex Dichroic Feed System
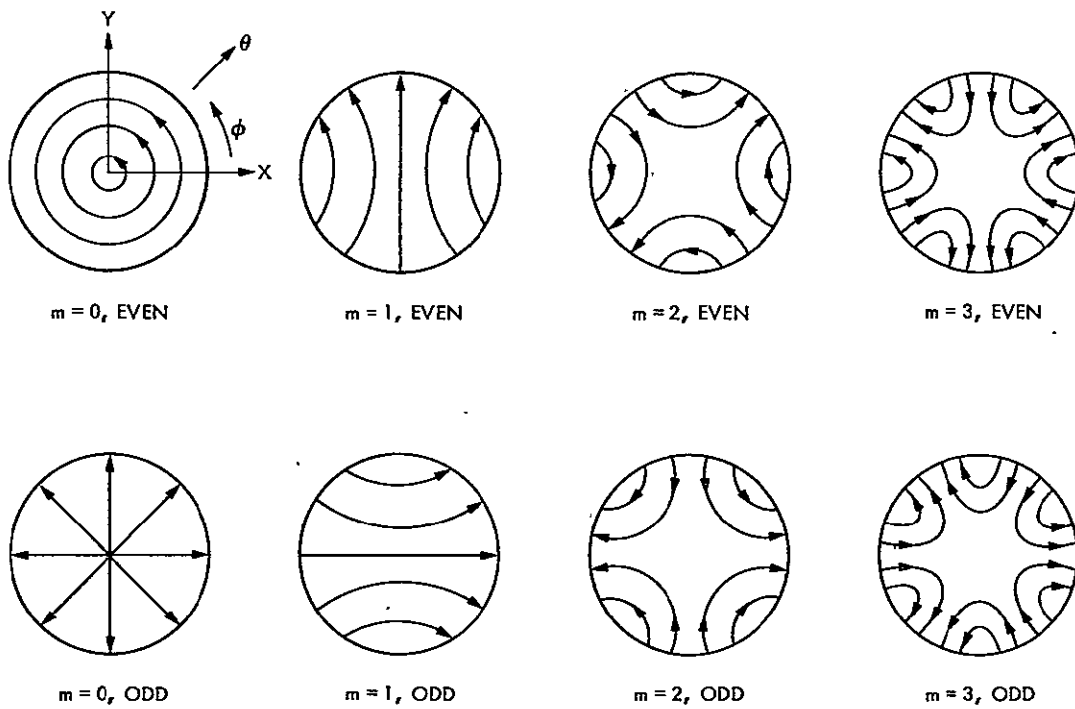
Figure 4-4. Field Lines, Fourier Components

will create a negative field pattern whose voltage peak V_b relative to the voltage peak V_m of the original main aperture pattern (Ref. 4-9) is

$$\frac{V_b}{V_m} = 2\left(\frac{D_b}{D_m}\right)^2$$

where

D_b = diameter of blocking aperture

D_m = diameter of main aperture

Therefore, the resultant central blocking efficiency η_c for the tapered illumination aperture is

$$\eta_c = \left[1 - 2\left(\frac{D_b}{D_m}\right)^2\right]^2$$

Similarly for a uniformly illuminated aperture, the efficiency η_c due to central blockage is

$$\eta_c = \left[1 - \left(\frac{D_b}{D_m}\right)^2\right]^2$$

The blocking of feed support spars or other structures in the field of view must also be included. Typical large short-focus micro-wave reflectors have feed support area blockages ranging from 6% down-wards. A frequently applied approximation is to view the aperture shadowing due to a simple solid feed support spar as consisting of two parts: a portion intercepting the planewave radiation and a portion intercepting the spherical (focusing) wave radiation. Taken together, the two parts frequently add to an approximate "pie-slice" shadow on the aperture. To the degree the shadow is a perfect wedge shape, the relationship

$$\eta_w = \left(1 - \frac{A_B}{A_o}\right)^2$$

is perfect. A_B/A_O is the ratio of the spar area to the main reflector area, and the squared effect is due to area and power being blocked and scattered, respectively. Thus, the effect of 6% area blockage (due to spars) is seen to result in a 12% effect, approximately.

The total blocking is then the product

$$\eta_{BL} = \eta_c \eta_w$$

G. SURFACE TOLERANCE EFFICIENCY

Any reflector surface has irregularities which depart from an ideal surface and impact the electromagnetic reflection performance. Loss of axial gain, energy scattered into sidelobes (or, alternately, increased receiving susceptibility to off-axis radiation), and reduction of far-field main beam efficiency are the major effects. To a lesser degree, one expects (in the general case) cross-polarization to be impacted as well.

There are perhaps three major categories of scale sizes (scale implying lateral extent) associated with surface irregularities: large scale (low spatial frequency), such as is produced by an off-axis feed or other systematic macrostructure effect, which may manifest itself as primarily a beam squint (and is most often largely correctable by focusing the feed); medium scale, such as that due to a repetitive error in each segment of a panel-type antenna; and small scale (high spatial frequency) antenna microstructure effects such as those due to frequently recurring random bumps or dents.

For really large reflector antennas consisting of a support frame and petaled reflecting skins, medium to large scale-size errors are frequently a function of environmental effects (gravity, thermal), while small scale-size errors are most often the result of manufacturing imperfections. For large space antennas, one immediately suspects that the effects might tend to be primarily of large scale-size type (due to thermals, for example). Active figure control of large, continuous surfaces is a frequently suggested solution to such problems and is a topic well beyond the scope of this report, except to observe that the complexity of such subsystems might approach that associated with a discrete phased array of comparable size. One should expect that simple feed (or secondary reflector) focusing, coupled with means to keep the far-field beam pointed properly, would recover a large fraction of the performance lost due to macrostructure effects. This is certainly the experience with large gravity antennas, and should be the case with space antennas.

In the theory of antenna performance as a function of surface errors, the error at one point in a continuous surface implies that the error will also exist in the adjacent area around the point, since the error is frequently due to a misshaped or misaligned panel or a bump.

According to Ruze, the average size of the surface error in lateral extent is called the correlation interval C (Ref. 4-10). This means that, on the average, C is the distance where the errors are essentially independent, i.e., are completely correlated over a diameter of 2C and completely uncorrelated for larger distances. These error regions have little effect on the amplitude distribution, but the phase errors affect the sidelobe levels of the perfect reflector. A broad, scattered field pattern is reflected from the errored surface, whose beamwidth is inversely proportional to the size of the average correlated region, in wavelengths. Thus, large correlation regions of large, smooth reflectors scatter the energy with greater directivity (in the vicinity of the main beam), affecting near-in sidelobes, while rough reflectors (small C) scatter more diffusely, affecting the wide-angle sidelobe level. For the same small phase errors, the relative magnitude of the axial scattered field from Ref. 4-10 is

$$\frac{V_s}{V_m} = \frac{1}{\eta} \left(\frac{2C}{D}\right)^2 \overline{\delta^2}$$

where

V_s/V_m = relative magnitude of the scattered field

η = aperture efficiency

$2C$ = correlation diameter

D = diameter of reflector

$\overline{\delta^2}$ = mean-squared phase error, rad^2

Thus, the scattered field with large C will have a greater effect on gain loss than small C for the same mean-squared phase error.

The relationship for the loss in gain has also been worked out by Ruze. For small errors, simplified expressions for efficiency were obtained for small and large correlation intervals, as follows:

$$\eta_S = \frac{G}{G_o} \approx 1 - \frac{3}{4} \overline{\delta^2} \frac{C^2 \pi^2}{\lambda^2}, \text{ when } \frac{C}{\lambda} \ll 1$$

and

$$\eta_S = \frac{G}{G_o} \approx 1 - \overline{\delta^2}, \text{ when } \frac{C}{\lambda} \gg 1, \text{ and } \lambda \text{ is the wavelength}$$

Ruze, in a 1966 paper, worked out an improved model for reasonable tolerance losses and for the usual case of correlation intervals large compared to a wavelength (Ref. 4-11):

$$\eta_S = \frac{G}{G_o} = \exp - \left(\frac{4\pi\varepsilon}{\lambda}\right)^2$$

where ε is the rms surface error, in the same units as λ. Figure 4-5 is a plot of gain loss as a function of rms surface tolerance, in wavelengths. It is suggested that the region of safe applicability of this figure is for small rms tolerances (less than about 7% of a wavelength).

Figure 4-6 uses the same improved model as previously plotted, this time covering the frequency band of interest in this report. Again, use of the figure for large tolerances (gain losses greater than about 3 dB) is not recommended.

Figure 4-7 shows generally the radiation pattern effects due to surface tolerance on a rather small reflector.
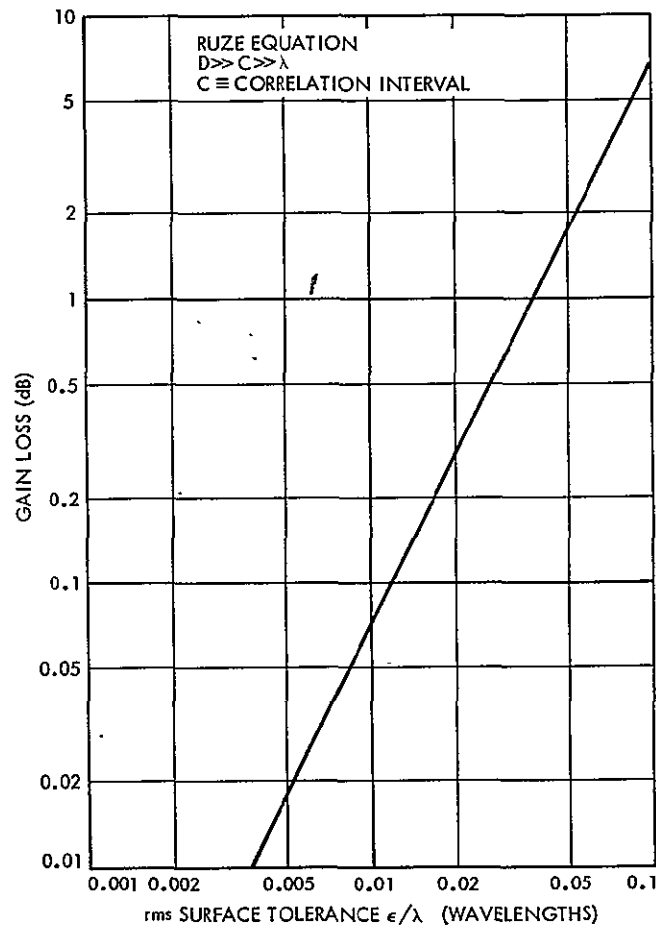

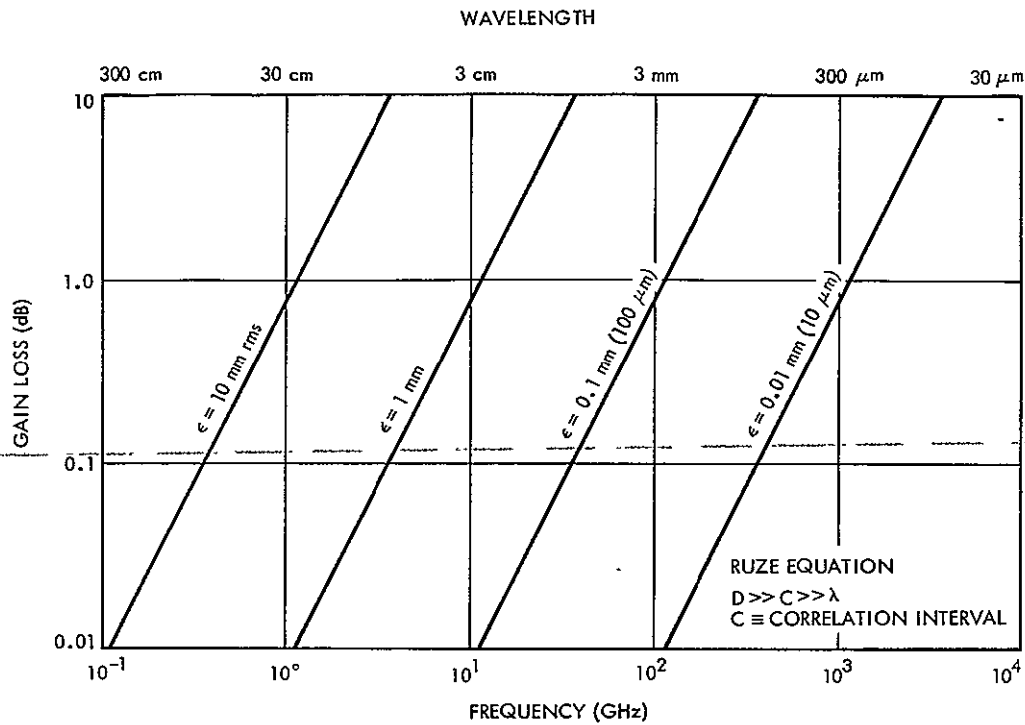Figure 4-5. Gain Loss as a Function of Surface Tolerance

WAVELENGTH

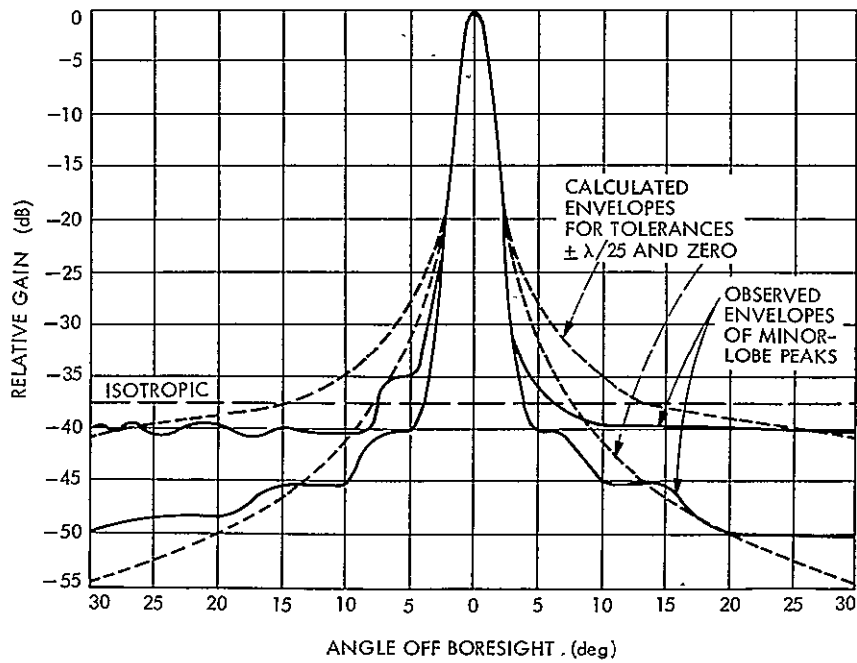Figure 4-6. Gain Loss as a Function of Frequency
and Surface Tolerance

Figure 4-7. Surface Tolerance Effects on
Radiation Patterns

H.   ANTENNA NOISE TEMPERATURE

When electromagnetic energy, at any frequency, strikes a body, some of the energy is transmitted through the body, some is reflected, and the remainder is absorbed. Those portions of energy that are transmitted or reflected do not increase the physical temperature of the body. However, the energy that is absorbed increases the molecular activity and causes an increase in the physical temperature of the body. If all the energy is absorbed, the body is called a blackbody, and its absorption coefficient α is equal to 1. Since the body must be in thermal equilibrium, all the energy that is absorbed will be emitted. Consequently, any matter which has absorptive properties emits energy over the whole microwave spectrum, the spectral distribution being a function of the physical temperature of the body and its absorption coefficient.

The energy that is emitted in the frequency band of interest is noise. The total noise power available from the radiating body (Refs. 4-12 and 4-13) is

$$P = \alpha k T_p B$$

where

α = absorption coefficient ≤ 1

k = Boltzmann's constant (1.3806×10^{-23} J/K)

T_p = physical temperature of the body, K

B = bandwidth, Hz

The effective noise temperature of an antenna can be defined as the temperature at which an equivalent resistor must be maintained to produce the same noise power, if it replaces the antenna. Therefore, the noise temperature of the antenna, in Kelvins, is:

$$T_{ANT} = \frac{w}{k}$$

where w is the power available per unit bandwidth (W/Hz), and k is Boltzmann's constant, as before.

The noise that is received at the antenna terminals is due to the summation of blackbody radiation, as discussed above, from the various noise emitters surrounding the antenna, plus internal noise contributions from the reflector, feed, and transmission line dissipative attenuations (other α-terms, as above).

The noise emitters are the earth and sea absorption, galactic
noise, isotropic background radiation, quantum noise, and, for terres-
trial antennas, absorption due to the oxygen and water vapor in the
earth atmosphere. Any antenna sees a minimum of 2.7 to 3.0 K isotropic
background radiation. Above 60 GHz, the quantum noise, as seen by an
ideal coherent receiver, has emerged above the background noise and
ultimately becomes proportional to frequency.

Galactic noise, mainly due to synchrotron radiation, falls
rapidly with increasing frequency and is strongest in the direction of
the center of the galaxy. There is also a quantum limit on the detector
sensitivity, which becomes the primary factor as one approaches optical
frequencies. The noise level for an ideal coherent receiver of elec-
tromagnetic waves (Ref. 4-14) is

$$w = \frac{h\nu}{e^{h\nu/kT} - 1} + h\nu$$

where

w = noise power, W/Hz

h = Planck's constant = 6.626×10^{-34} J-s

k = Boltzmann's constant, as before

ν = frequency, Hz

T = temperature of field of view, K

The first term is the thermal noise due to finite temperature,
and the second is wholly quantum-mechanical in origin. At low fre-
quencies, where $h\nu/kT \ll 1$, $w \approx h\nu + kT \approx kT$, which is independent of
frequency. At high frequencies, such that $h\nu/kT \gg 1$, the thermal noise
term disappears and $w \approx h\nu$, directly proportional to frequency.

As we show above, it has been customary to define system noise
in terms of an equivalent noise temperature $T \equiv w/k$; then the noise
temperature of an ideal receiver becomes

$$T = \frac{h\nu}{k} \left(\frac{1}{e^{h\nu/kT} - 1} + 1 \right)$$

Figure 4-8 shows the general level of minimum received noise associated
with galactic, background, and quantum noise sources and the earth atmo-
sphere absorption plotted as brightness temperature as a function of
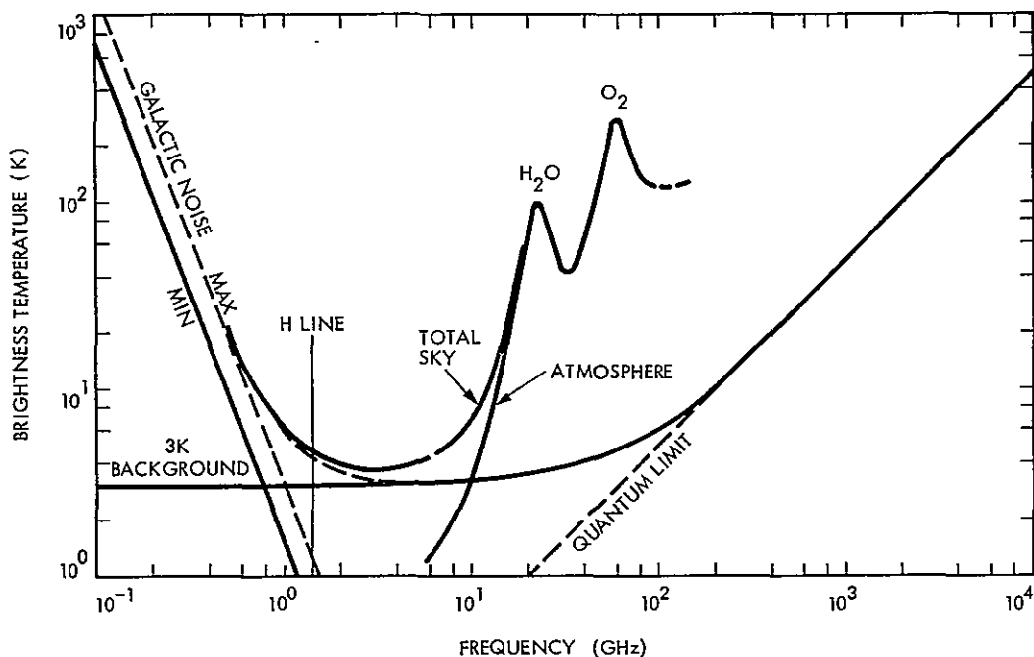
Figure 4-8. Noise Temperature for Coherent Receivers

frequency. We see that for outward viewing (space) applications, the
three noise sources (galactic, 3-K background, and quantum noise) define
a broad low-noise region of the radio spectrum from approximately 1 to
100 GHz, while for terrestrial applications, looking toward the sky, the
available low-noise spectrum is reduced to approximately 1 to 10 GHz.

The overall antenna temperature may be expressed by

$$T_{ANT} = \sum_{n=1}^{p} A_n T_n$$

where A_n is the fraction of the total power contained in the nth sector
of the solid angle and T_n is the average brightness temperature of the
absorbing medium as seen by this nth sector.

For a large reflector antenna, the pattern can be divided so that
the main beam and near-in sidelobes see the brightness temperature in
the direction of interest, while the energy in the wide sidelobes,
spillover, and energy scattered from the spar structure as well as
energy transmitted through the reflector (if any) may each see different
average brightness temperatures.

I.   DISSIPATIVE LOSSES

Excluding the very-high-loss (1 dB or more) systems, even the very-low-loss reflector systems require careful attention to dissipative losses for many applications. When low-noise-level reception is the key system requirement (most deep space viewing applications), small dissipative losses (tenths of decibels) may dramatically reduce system sensitivity. This occurs (as seen in Section IV-H) if the physical temperature of the absorber/emitter is, say, 300 K. In fact, for this physical temperature, noise is added at a rate of 6.7 K per 0.1 dB of dissipative component (not overall insertion) loss. Since deep space antenna systems operating in the approximate band 1 to 100 GHz may achieve total noise levels of 10 K or less, a negligible (for other systems) 0.1 dB of tertiary dissipation will in fact cause nearly 3 dB loss of sensitivity for a coherent receiver. Thus, electromagnetic reflection and conduction losses must be very carefully handled and minimized in these systems. On the other hand, most earth viewing applications will have relatively high-noise-level reception as an inescapable characteristic, due to the radiometric temperature of the earth, and a few percent (tenths of decibels) of dissipative loss will be experienced as simply a signal loss, not the additional, highly performance degrading noise increase.

J.   FAR-FIELD RADIATION PATTERNS

In this, the final discussion of key performance parameters, we conclude by examining some of the observables in the secondary (far-field) radiation patterns associated with large dual-reflector antennas. Figure 4-9 shows a face-on view of the measured copolarized far-field radiation pattern of a 200-wavelength-diameter Cassegrain ground antenna. The main beam is nearly perfectly centered on (0, 0), and each contour interval is a step of -3 dB. The figure shows the azimuthal variation in sidelobe level caused primarily by the four-legged spar structure associated with the antenna. This typical effect is illustrated here as the microwave equivalent of optical telescope secondary mirror support "spider" effects on star images. Viewing this figure nearly edge-on is helpful to fully appreciate the effect.

Figures 4-10 and 4-11 show several additional calculated features of the secondary pattern. Figure 4-10, for the same 200-λ antenna as above, also shows a lobe of forward spillover (at 20 deg off boresight) due to the Cassegrain configuration. Also, beyond 120 deg, the response generally decreases. Similar behavior is seen in Fig. 4-11 for a 500-λ ground antenna.

Figures 4-12 and 4-13 examine the same calculated data as before, but with a slightly different viewpoint. Here we can see that the calculated diffraction pattern of the unblocked aperture alone is not adequate to describe the wide-angle response. In these cases, the wide-angle response is still dominated by spar blocking, and to a lesser degree by spillovers. (The lobes at ±120 deg are due to rear spillover.)

CROSS ELEVATION (deg)
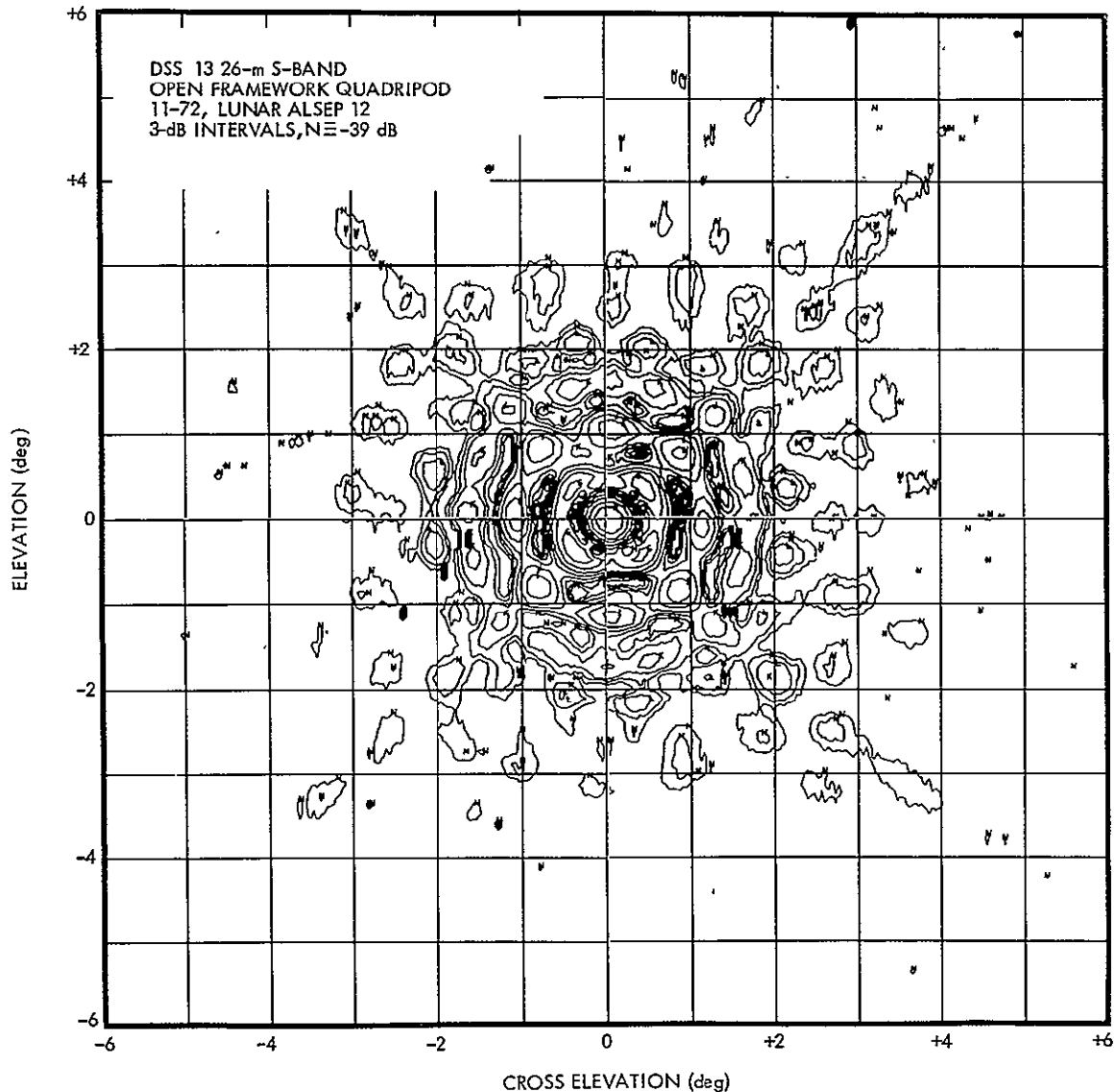
Figure 4-9. Antenna Pattern Contour

For both antennas presented, surface tolerance precision is sufficiently high (ε/λ is approximately 0.01) to have negligible impact. Also, there are no significant reflector leakage terms. Were these additional effects to be present, as might be typical of a lightweight space antenna, the wide-angle response might be significantly higher. Measurements of wide-angle effects of these ground antennas (albeit at close range) have roughly confirmed the calculations seen in Figs. 4-10 through 4-13.

In summary, several contributors to the far-field secondary patterns of a large reflector antenna must be evaluated to obtain the complete response; the diffraction pattern is but one of these. Occasional proposals for "reduced" or "low" sidelobe antennas must necessarily be viewed with these additional factors in mind.

Figure 4-10. Calculated Radiation Pattern Envelopes,
D/λ = 200

Figure 4-11. Calculated Radiation Pattern Envelopes,
D/λ = 500

Figure 4-12. Calculated Radiation Patterns,
D/λ = 200

Figure 4-13. Calculated Radiation Patterns,
D/λ = 500

SECTION V

USER'S INTEREST IN KEY PERFORMANCE PARAMETERS

With the background of material from the previous sections, we complete this report by touching, in a very broad way, on a few space applications employing large antennas. The goal h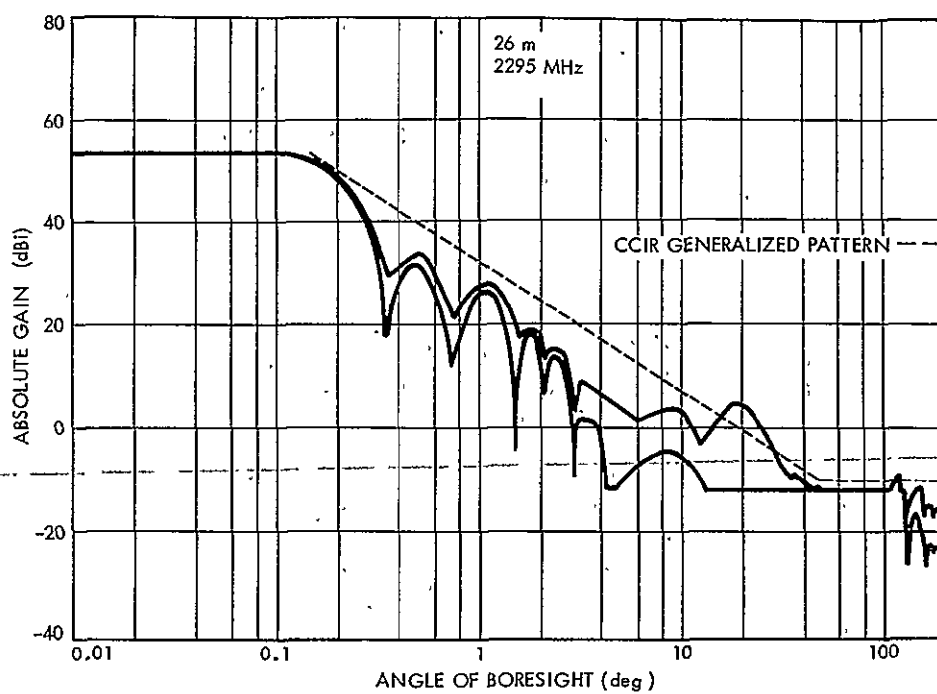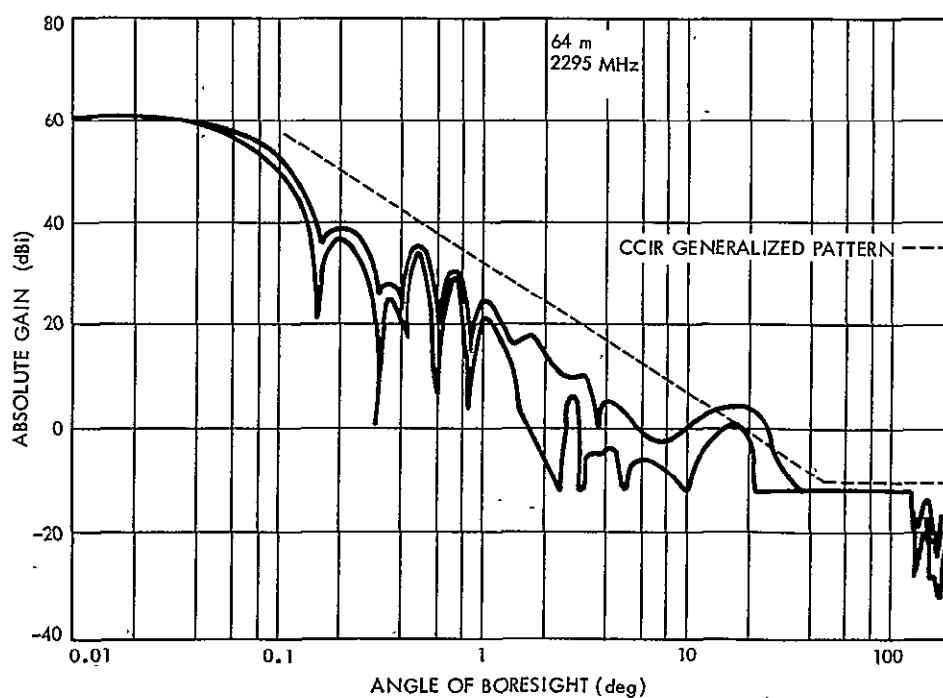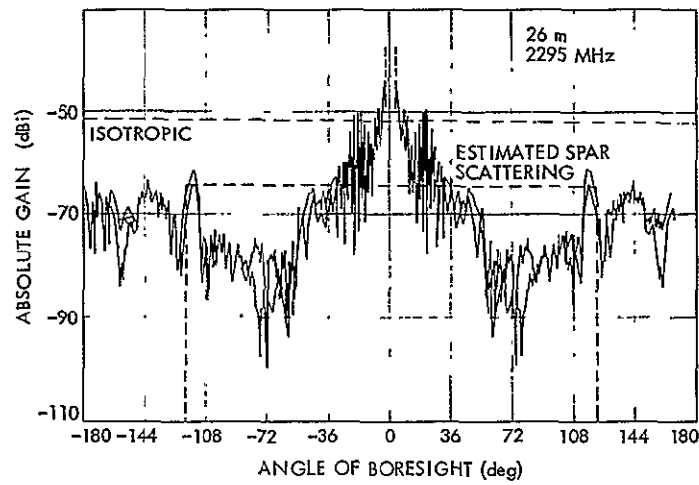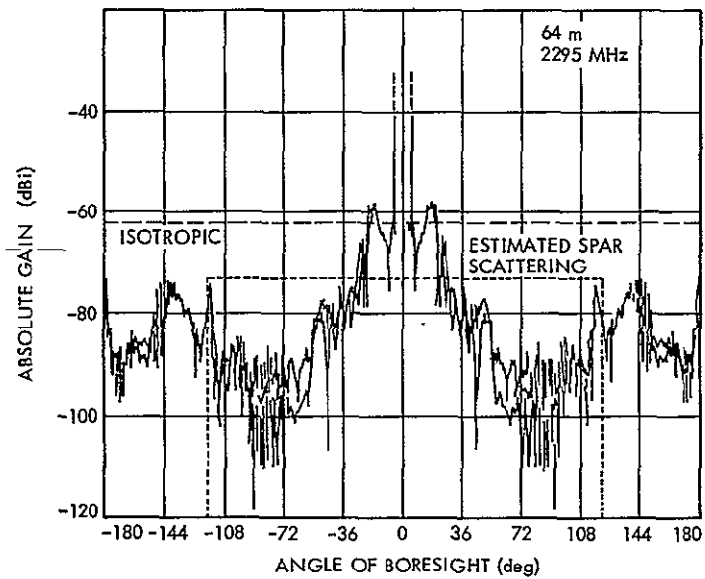ere is to show how the application determines the selection of an antenna type and configuration, and again, to attempt to develop and maintain overall perspective. We first divide the applications into outward-looking (space) and downward-looking (earth). Next, the low receiving noise levels usually associated with outward-looking missions is identified as the key to forming the first of two broad classifications:

(1) Outward-looking (low noise)

(2) Downward-looking (high noise)

(a) Radiometry

(b) Communications

A. OUTWARD-LOOKING

Outward-looking antennas are contemplated for near-term applications such as millimeter, infrared, and ultraviolet astronomy, ultralong baseline interferometry, as well as probable future applications such as deep space probe tracking, the proposed search for extraterrestrial intelligence (SETI), planetary communications, radioastronomy (particularly in the submillimeter spectrum), and undoubtedly others. The antenna requirements for these applications will typically include high aperture efficiency, wide bandwidths, and very low noise (at the longer wavelengths at least), with limited or no scan capability required. One would expect the traditional low-dissipative-loss reflector types to be applied in these cases, with probable limited use of hybrid reflectors for a few multibeam applications. The proposed search for extraterrestrial intelligence mission, for example, might benefit from multiple beams inasmuch as search time could. possibly be reduced. Scanning technology and high beam efficiency (as contrasted with high area efficiency) do not appear to be vital to the success of most (if any) of these activities. On the other hand, clear-aperture (offset) designs, especially at the longer wavelengths, may be required from a radiation pattern viewpoint (RFI-immune designs), especially for the sensitive wideband search mission. The short-wavelength applications (millimeter, IR, UV) would most likely continue to be best served with conventional medium-focal-length symmetric reflector optics.

B. · DOWNWARD-LOOKING

Downward-looking antennas are seen for near-term applications such as significant further exploitation of earth observation radiometry, public and private sector and general communications, with probable future applications in RFI monitoring, and downward-looking multi-frequency (meteorological and other) radars. Certainly, microwave power transmission is a unique downward-looking (active) application, and will be mentioned here only in passing. The antenna requirements for the earth-looking radiometry, RFI monitoring, and filled and synthetic-aperture radar applications will typically be resolution or "footprint" size and associated beam quality (beam efficiency), scanning, scanning rates, and wideband or multifrequency capability. In the public and private sector and general communications applications, the primary need appears to be for multibeam (and closely related contour-beam) capability.

Common to all earth-looking applications is the radiometric antenna temperature (noise) from the earth surface and/or atmosphere. This characteristic maps into unavoidable medium- or high-quiescent-noise-level systems not requiring the ultralow dissipative losses nor low-noise amplifiers associated with the very sensitive outward-looking applications. For some earth-looking communications users, only average requirements on area and beam efficiency might be expected, although RFI monitoring and frequency reuse (through multibeam) could ultimately place strong requirements on at least the latter.

Needless to say, we will see a great variety of antenna types applied to the wider variety of downward-looking tasks. These will almost certainly include some pure arrays, for beam scanning agility, with probable heavy use of hybrids, both array-fed reflectors and lenses, depending on bandwidth and/or multifrequency needs. Those applications needing very wide bandwidths and wide but slow scan, but with a well formed beam or beams, may ultimately be best served with an oversized spherical reflector, highly underilluminated, and therefore fitted with relatively simple feeds.

A very broad and undetailed scenario might look as follows. Deployable antennas (focusing reflectors and other types) will most likely be widely applied and tend to economically service a variety of important but perhaps nonlimiting (in the sense of pushing performance) applications. Limiting applications requiring very high beam efficiency (i.e., very precise surfaces and/or use at very short wavelengths) are viewed as difficult to realize with present-day deployable antenna technology. Such limiting applications will most likely be handled with rigid space-erectable antennas.

REFERENCES

1-1. *Proceedings of the IEEE*, Special Issue on Satellite Communications, Vol. 65, No. 3, March 1977.

3-1. Oliner, A. A., and Knittel, G. H., *Phased Array Antennas*, Artech House, Dedham, Mass., 1972.

3-2. Hansen, R. C., *Microwave Scanning Antennas*, Vol. II, Academic Press, New York, 1964.

3-3. Stark, L., "Microwave Theory of Phased-Array Antennas - A Review," *Proceedings of the IEEE*, Vol. 62, No. 12, pp. 1661-1701, December 1974.

3-4. Rotman, W., and Turner, R. F., "Wide-Angle Microwave Lens for Line Source Applications," *IEEE Trans. on Antennas and Propagation*, Vol AP-11, pp. 623-632, November 1963.

3-5. Spencer, R. C., Slettin, C. J., and Walsh, J. E., "Correction of Spherical Aberration by a Phased Line Source," *Proceedings of the National Electronics Conference*, Vol. 5, Chicago, 1950.

3-6. Galindo, V., "Design of Dual Reflector Antennas with Arbitrary Phase and Amplitude Distribution," *IEEE Trans. on Antennas and Propagation*, Vol. AP-12, pp. 403-408, July 1964.

3-7. Williams, W. F., "High Efficiency Antenna Reflector," *Microwave Journal*, Vol. 8, pp. 79-82, July 1965.

3-8. Chu, T., and Turrin, R. H., "Depolarization Properties of Offset Reflector Antennas," *IEEE Trans. on Antennas and Propagation*, Vol. AP-21, pp. 339-345, May 1973.

3-9. Galindo, V., and Mittra, R., "Synthesis of Offset Dual Shaped Reflectors With Arbitrary Control of Phase and Amplitude," accepted for publication in the *IEEE Trans. on Antennas and Propagation Symposium* to be held in June 1977.

3-10. Kumazawa, H., and Karikomi, M., "Multiple-Beam Antenna for Domestic Communication Satellites," *IEEE Trans. on Antennas and Propagation*, Vol. AP-21, pp. 876-878, November 1973.

3-11. Rao, B.L.J., "Bifocal Dual Reflector Antenna," *IEEE Trans. on Antennas and Propagation*, Vol. AP-22, pp. 711-714, September 1974.

3-12. Cha, A., and Galindo, V., Private Communication.

4-1. Kraus, J. D., *Antennas*, McGraw-Hill Book Company, New York, 1950.

4-2. Baars, J.W.M., "The Measurement of Large Antennas with Cosmic Radio Sources," *IEEE Trans. on Antennas and Propagation*, Vol. AP-21, pp. 461-474, July 1973.

4-3. Ko, H. C., "Radio-Telescope Antenna Parameters," _IEEE Trans. Military Electron._, Vol. MIL-8, pp. 225-232, July-October, 1964.

4-4. Nash, R. T., "Beam Efficiency Limitations of Large Antennas," _IEEE Trans. Military Electron._, Vol. MIL-8, pp. 252-257, July-October, 1964.

4-5. Wood, P. J., "Crosspolarization with Cassegrainian and Front-Fed Reflectors," _Electronics Letters_, Vol. 9, No. 25, pp. 597-598, December 1973.

4-6. Davis, R. T., "Satellite Communication; The Search for More Bandwidth," _Microwaves_, Vol. 14, pp. 14-18, January 1975.

4-7. Jacobsen, J. J., "On the Cross Polarization of Asymmetric Reflector Antennas for Satellite Applications," _IEEE Trans. on Antennas and Propagation_, Vol. AP-25, pp. 276-283, March 1977.

4-8. Potter, P. D., "S- and X-Band RF Feed System," in _The Deep Space Network_, Technical Report 32-1526, Vol. VIII, Jet Propulsion Laboratory, Pasadena, Calif. pp. 53-60, April 1972.

4-9. Hannan, P. W., "Microwave Antennas Derived from the Cassegrain Telescope," _IEEE Trans. on Antennas and Propagation_, Vol. AP-9, pp. 140-153, March 1961.

4-10. Ruze, J., _Physical Limitations on Antennas_, Report 248, Massachusetts Institute of Technology, Research Laboratory of Electronics, October 1952.

4-11. Ruze, J., "Antenna Tolerance Theory - A Review," _Proceedings of the IEEE_, Vol. 54, No. 4, pp. 633-640, April 1966.

4-12. Steinberg, J. L., and Lequeux, J., _Radio Astronomy_ (translated by R. N. Bracewell), McGraw-Hill Book Company, New York, 1963.

4-13. Kraus, J. D., _Radio Astronomy_, McGraw-Hill Book Company, New York, 1966.

4-14. Young, L., _Advances in Microwaves_, Vol. 5, Academic Press, New York, 1970.

A-1. Ruze, J., "Lateral-Feed Displacement in a Paraboloid," _IEEE Trans. on Antennas and Propagation_, Vol. AP-13, pp. 660-665, September 1965.

A-2. Galindo, V., Lee, S. W., and Mittra, R., "Synthesis of a Laterally Displaced Feed for a Reflector Antenna with Application to Multiple Beams and Contoured Patterns," accepted for publication in the _IEEE Transactions on Antennas and Propagation Symposium_ to be held in June 1977.

A-3. Rudge; A. W., and Withers, M. J., "New Technique for Beam Steering With Parabolic Reflectors," Proc. IEE, Vol. 118, No. 7, pp. 857-863, July 1971

A-4. Fitzgerald, W. D., Limited Electronic Scanning with a Near-Field Cassegrainian System, Report 484, Lincoln Laboratory, Mass. Inst. Tech., Lexington, September 1971.

A-5. Stein, S., "On Cross Coupling in Multiple-Beam Antennas," IEEE Trans. on Antennas and Propagation, Vol. AP-10, pp. 548-557, September 1962.

A-6. Williams, W. F., Antenna Pattern Contouring Study, Jet Propulsion Laboratory, Private Communication.

B-1. Woo, R., "A Multiple Beam Spherical Reflector Antenna," JPL Quarterly Technical Review, Vol. 1, No. 3, pp. 88-96, October 1971.

B-2. Li, T., "A Study of Spherical Reflectors as Wide-Angle Scanning Antennas," IRE Trans. Antennas and Propagation, Vol. 7, pp. 223-226, 1959.

B-3. Spencer, R. C., "Studies of the Focal Region of a Spherical Reflector: Geometrical Optics," IEEE Trans. Antennas and Propagation, Vol. 16, pp. 317-324, May 1968.

APPENDIX A

HYBRID SYSTEMS

Hybrid systems, consisting of a small array of elements feeding various microwave optical systems, form a promising class of antennas for limited scan applications. Of course, the number of control elements is drastically reduced with respect to a phased array of the same overall gain. The scanning capability may be enhanced compared to that of the associated reflector or lens, but to only a fraction of that available from a full phased array. With respect to reflectors, the usual method of scanning a paraboloid has been to radially displace a single feedhorn from the focal point, which causes both linear and cubic phase terms to appear across the aperture. The linear phase shift term causes the desired (undistorted) shift of the main beam, while the cubic term causes a slight shift in the opposite direction and considerable beam distortion. The beam becomes wider, and the sidelobe close to the main beam in the direction opposite of scan (called the coma lobe) rapidly increases. An example given by Ruze shows a 1.0-dB gain loss with a scan of ±4 beamwidths, with the coma lobe significantly increased (Ref. A-1).

A typical and moderately successful technique for reducing pencil beam distortion resulting from scanning the beam away from the focus is to control the feed illumination more carefully so as to partially reduce the aperture phase errors. An effective approach to accomplishing this with an array feed is to combine several overlaying (clustered) feeds for each pencil beam radiated. The matrix distribution system for each cluster of feeds is designed appropriately to minimize the distortion normally present for the feedhorn central to the cluster of feeds. A typical arrangement is that which occurs in an equilateral triangular feed array with six cluster "compensatory" feeds surrounding each feed central to the cluster (Fig. A-1). Recently developed synthesis methods (Ref. A-2) have been used to partially correct the distortion in the scanned beam. The use of six compensatory feeds in the manner of Fig. A-1 enabled the sidelobes to be reduced from -13 to -19 dB. The sidelobes for the undistorted beam on focus were a maximum of -26 dB. The use of additional (secondary) "rings" of cluster compensatory elements surrounding a central cluster does not materially improve the pattern unless the feed array elements are very closely spaced ($\leq \lambda/4$). Very close spacing does lead to supergaining and narrow bandwidth.

Since the coma phase error is the major deterrent to scanning a paraboloid, several methods have been attempted to further reduce the effect. In general, this is accomplished by reproducing at (or in) the feed system a scaled-down copy of the aperture distribution of the main reflector. If the distribution in the feed matches the main aperture, then phased array beam steering techniques can be utilized in the feed array. Since array antennas have no coma phase errors, scanning of the feed array to shift the main beam should produce beams with no coma sidelobes. As Rudge has pointed out, the fields in the focal region of a parabola are a Fourier transform of the aperture field of the paraboloid (Ref. A-3). Therefore, an inverse Fourier transform of the focal region fields would recreate the original aperture distribution. If the focal region fields are sampled with an array of horn radiators, a device is needed which can transform the sampled fields to a set of
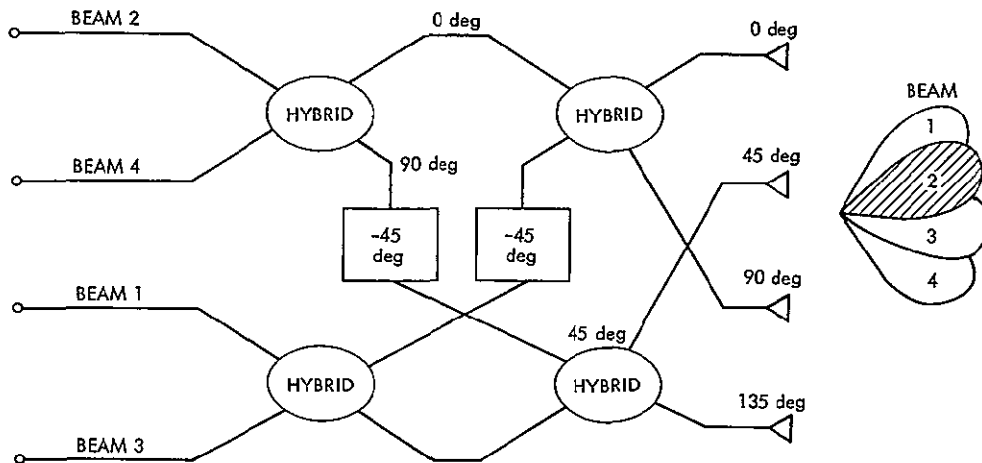
Figure A-2. Beam-Forming Butler Matrix

Figure A-3 shows the input terminals of a Butler matrix Fourier transformer fed with a typical phased array beam-steerable array network, which is shown schematically as a summing network with a phase shifter in each output port. This beam-steerable network may take the form of a Butler matrix or bootlace lens if multiple beams are desired. The discussion has been confined to beams distributed over a simple arc, so a two-dimensional array must be used both for the Fourier transformer and the beam steering device for two-dimensional coverage.

Using a Butler matrix-fed array, Rudge obtained ±15 beamwidths of scan with less than 0.5 dB reduction in system gain. The reflector used had an f/D of 0.5. The sidelobe level was not significantly changed. As discussed by Rudge, the size of the feed array is independent of size for the same f/D ratio, so blockage is not a problem. Although data are not available, this highly complex feed, with the resulting high ohmic loss, would probably cause the gain at boresight to be uniformly several decibels less· than could be obtained with the same reflector and a simple feed.

Another method of reducing the coma distortion in a reflector utilizes optical techniques to accomplish ·the Fourier transformation. Since the fields intercepted by the main parabolic reflector from a far-field source appear as a plane wavefront, the output of the Fourier transforming device near the focal point should also have the properties of a plane wavefront. Referring to Fig. A-4, which shows a Cassegrain antenna with a paraboloid subreflector having an f/D ratio the same as the main reflector, the fields scattered from the convex side of the subreflector form a collimated beam (i.e., a planar wavefront). A feed such as a planar array is placed to intercept the beam and is sized and located such that the distance is well inside the near field of the subreflector, so that the fields from the feed provide a match. This reflector system has been commonly referred to as a Near-Field (NF)
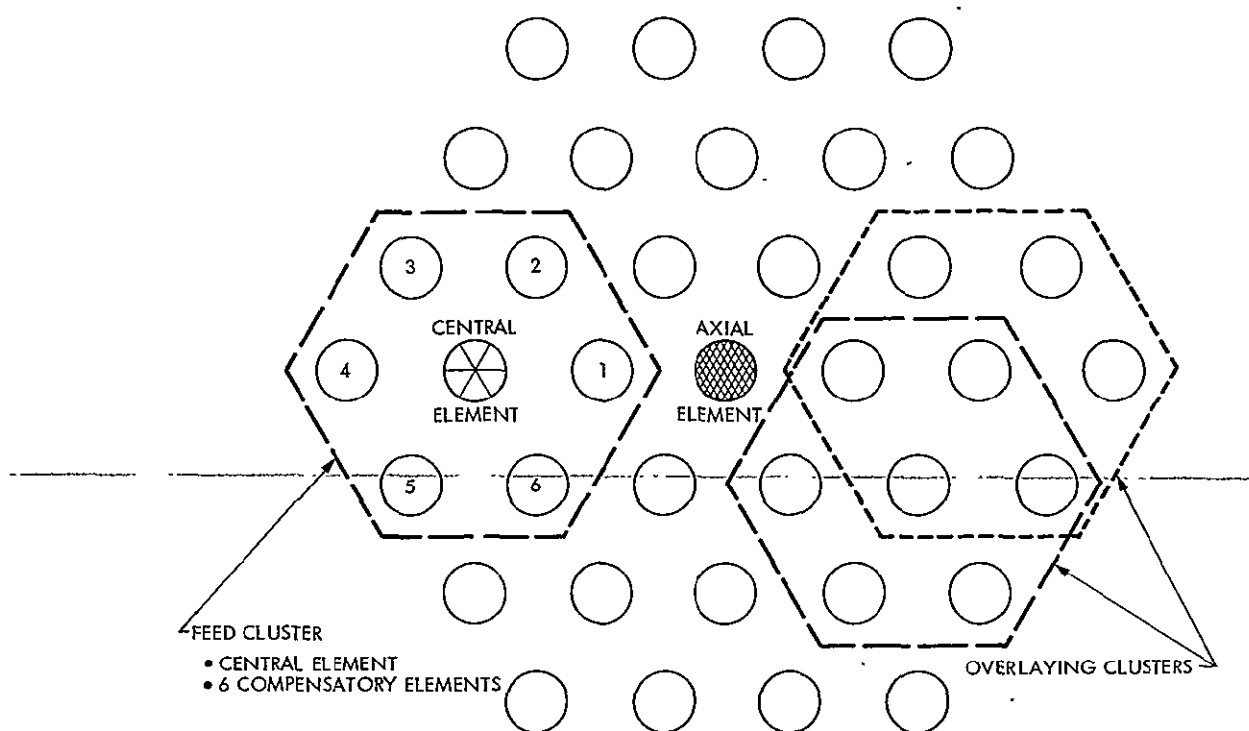
Figure A-1. Feed Array

voltages at its output which are similar to the main aperture fields.
A Butler matrix is a microwave network made up of 3-dB hybrid junctions
and appropriate fixed phase shifts which is capable of performing the
required transformation.

Figure A-2 shows an example of a four-element Butler matrix. As
may be seen, energy fed into the left upper port is divided equally
among the four output ports, with the phase taper shown, and no energy
leaves the other input ports. Feeding other input ports will provide
different phase tapers across the aperture. Connecting a small horn
radiator to each output port will then provide a (sin Nx)/(N sin x) beam
shape for each input, pointing in the direction dictated by the phase
taper and element spacing. It should be noted that N is the number of
radiators in a row or column and is equal to 4 in this example. If the
spacing between the horn radiators is set so that the peak of the pat-
tern formed by one input port occurs at the first null of the pattern
of the adjacent beam, then the patterns are orthogonal (i.e., they are
completely decoupled, and therefore the input ports are isolated). If
the four input ports are fed with equal power and the same phase, the
four narrow beams combine to form a fan beam with its phase center in
the array center. If the input ports are then fed with a progressive
phase, the phase center intentionally migrates away from the center of
the feed array. This is equivalent to radially displacing the feed in
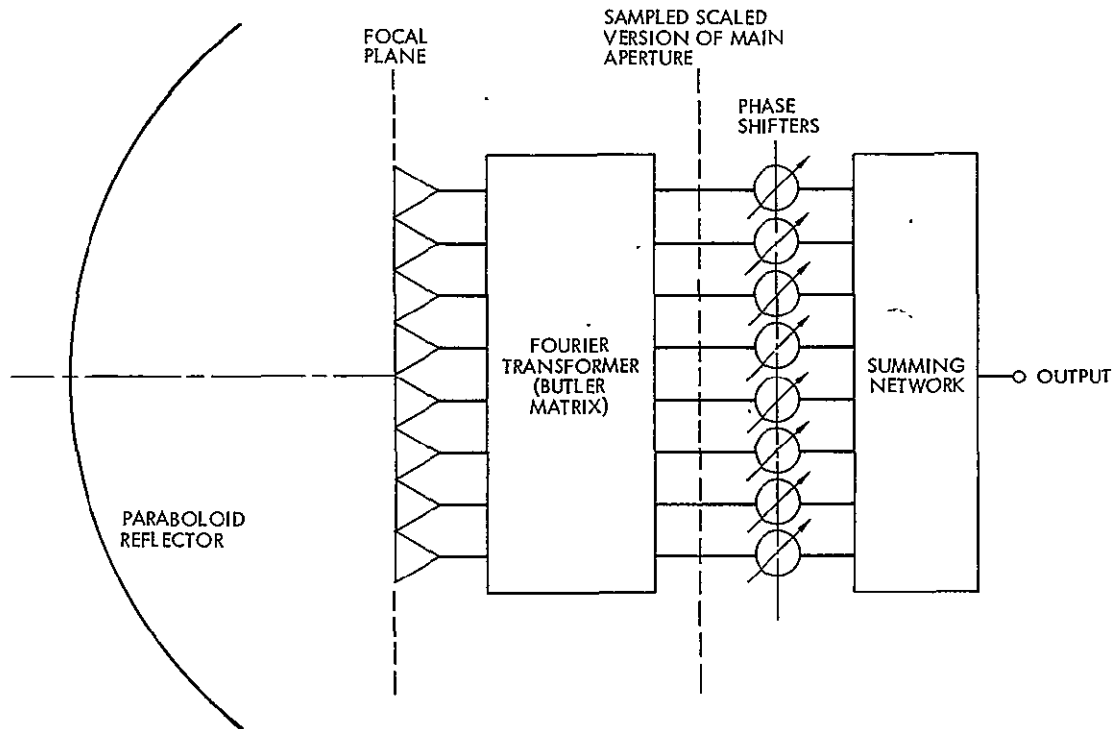a simple paraboloid, which will then scan the pencil beam.

7

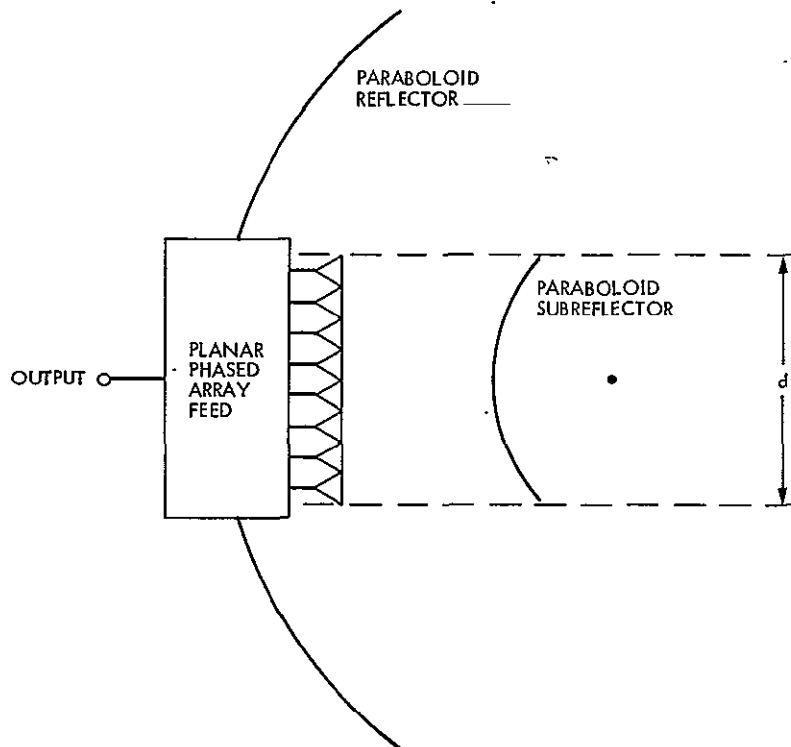Figure A-3. Beam Scanning Using Butler Matrix

Figure A-4. Beam Scanning Using Near-Field
Cassegrain

Cassegrain antenna. Using the anology given by Fitzgerald, one can visualize the mechanism involved in off-axis scanning by considering the NF Cassegrain as the limiting case of a conventional Cassegrain as the magnification becomes infinite (Ref. A-4).

Figure A-5 shows a conventional Cassegrain system of high ·magnification, where the feed is radially moved a distance Δ, causing the secondary beam to be scanned by an angle θ. By geometric consideration, tan β = (D/d) tan θ, where D is the diameter of the main reflector and d is the diameter of the subreflector. As the left-hand focal point is moved farther to the left, the hyperboloid subreflector becomes (in the limit) a paraboloid. The postulated feedhorn at infinity can be replaced with a planar phased array positioned noncritically at or near the vertex of the main reflector. Then, for small scan angles θ of the main beam, the phased array must produce a planar phase front, with scan angle β equal to

$$\beta \approx \frac{D}{d}\,\theta \approx M\theta$$

where θ is the main beam scan angle from boresight and M = D/d is the magnification ratio. For example, using a magnification of ten to one, the scan angle β requirements of the feed array will be 10 times greater than the scan angle of the main beam. The calculated and measured results obtained by Fitzgerald indicate a scanning loss of about 3 dB
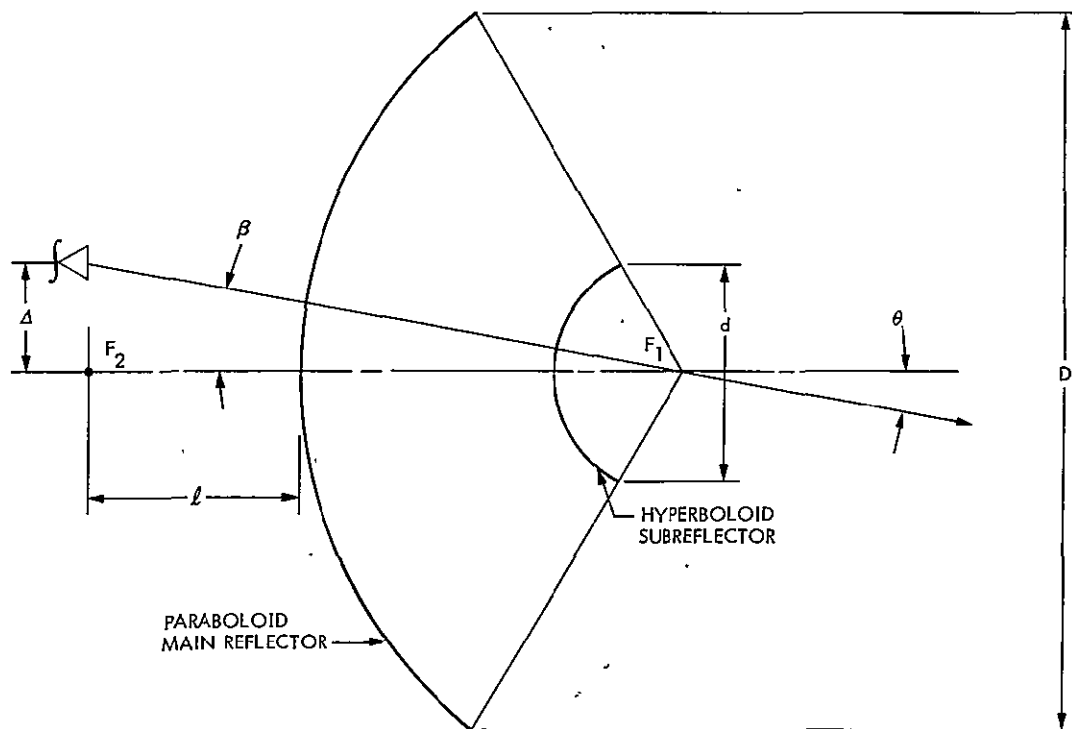

Figure A-5. Beam Scanning Using Simple Feed Displacement

when the main beam is scanned ±15 beamwidths. The pattern shows no problem with coma lobes, and the beam broadening (with -3 dB scan loss) is approximately 50%. The scan range is limited primarily by spillover of the subreflector. Also, the percentage subreflector blockage is fixed by the magnification ratio, so no decrease in blockage occurs by going to very large reflectors.

For hybrid systems with a dielectric or waveguide lens substituted for the parabolic reflector, the same feed systems as discussed for reflectors can be used. Some improvement results because of the elimination of feed blockage; on the other hand, complexity, weight, and perhaps the added dissipative loss of the lens as well must be considered. In view of the expected large dissipative losses in the feed system itself, however, the added loss due to the lens might be negligible.

1.   MULTIPLE-BEAM ANTENNAS

A multiple-beam antenna is a single antenna generating a number of simultaneous independent pencil beams, each pointing in a different direction. Each beam formed will thus have an independent input port in the transmit mode (or output port in the receive mode) of operation. These antennas may assume many different configurations, such as phased arrays, bootlace lenses, Butler arrays, etc. However, there are specific characteristics that are common to all such antennas. These characteristics pertain to the beam interactions in antenna gain, patterns, and feed port isolation. According to Stein, the input ports of a lossless feed system (lossless in the sense of power not cross-coupled into other beams or ports) can be decoupled only if the individual beam patterns are spatially orthogonal (Ref. -A-5).

The one-dimensional Butler array discussed above and the two-dimensional Butler array feeding a rectangular aperture with a rectangular element spacing are examples of such a lossless beam-forming network, generating orthogonal beams with (sin Nx)/(N sin x) radiation patterns. For these orthogonal patterns (with large N), the beam crossover level between adjacent patterns is at the $2/\pi = 0.6366$ voltage level (or -3.92 dB). If the patterns are not orthogonal, then the individual input beam ports will be coupled, or else the coupled power must be absorbed in the feed system to obtain input port decoupling. Either way, if nonorthogonal beams are used, the overall antenna gain will be reduced from the maximum aperture gain of a single-beam antenna.

If a lossless multiport antenna is used which has N orthogonal beams, then for the receiving case, full antenna gain can be simultaneously obtained on each of N output ports. Of course, if one transmitter is divided among N input ports for the transmitting case, the

effective radiated power (product of antenna gain and power input) will obviously be reduced by a factor of 1/N.

2. CONTOURED BEAM ANTENNAS

A recent study at JPL solved the general problem of determining the reflector focal region feed pattern required to generate a selected contoured far-field radiation pattern (Ref. A-6). In this study, the required far-field radiation contour was represented by a sequence of added orthogonal beams which could be available from an aperture the size of the selected antenna, $D/\lambda = 180$. The added beams then represent an attainable far-field contour pattern. The problem is then to determine what paraboloid prime focus feed pattern is required to develop the far-field contour pattern. A scattering calculation of the required contour pattern off the paraboloid and into the focal region would solve for the required focal region field. However, in practice, the scattering was done from the back of the paraboloid, because this results in the required focal point feed pattern (instead of the focal region field); this is a more useful objective for the feed system design engineer. Therefore, a spherical wave expansion of the complex contour beam (the sum of orthogonal beams) is made so that this pattern can be scattered from the back of the primary reflector, resulting in the required feed pattern. In a similar manner, a sequence of practical orthogonal beams can be added to obtain the feed pattern, and hence the resulting array illumination will be the feed required to generate the original selected contour pattern. A beam fit to the United States Eastern Time Zone (ETZ), for example, is shown in Figs. A-6, A-7, and A-8.

Figure A-6 presents the directions (dots) of a set of orthogonal beams and their magnitudes, which approximate the time zone as indicated. These beams are summed in phase. Figure A-7 represents the calculated feed pattern required to obtain the ETZ contour. Note that the polar coordinate Θ now extends to 80 deg, a figure representative of focal point feed angles, whereas the polar angles in Figs. A-6 and A-8 represent the scope of the footprint region seen from geosynchronous altitude. Figure A-8 checks the calculations by scattering the calculated feed pattern from the paraboloid in the normal manner. The result again presents the ETZ (as expected), which checks the procedure.

This technique will be useful in reducing spurious radiation into neighboring regions (perhaps countries) to acceptably low interference levels. It should be pointed out that the array feed that is developed for a contour pattern would not be restricted to just that one contour but could have its excitation distribution changed to obtain any selected contour. One envisions an array feed with a phase and amplitude control distribution network being commanded from a ground terminal to assume any previously calculated contour pattern.
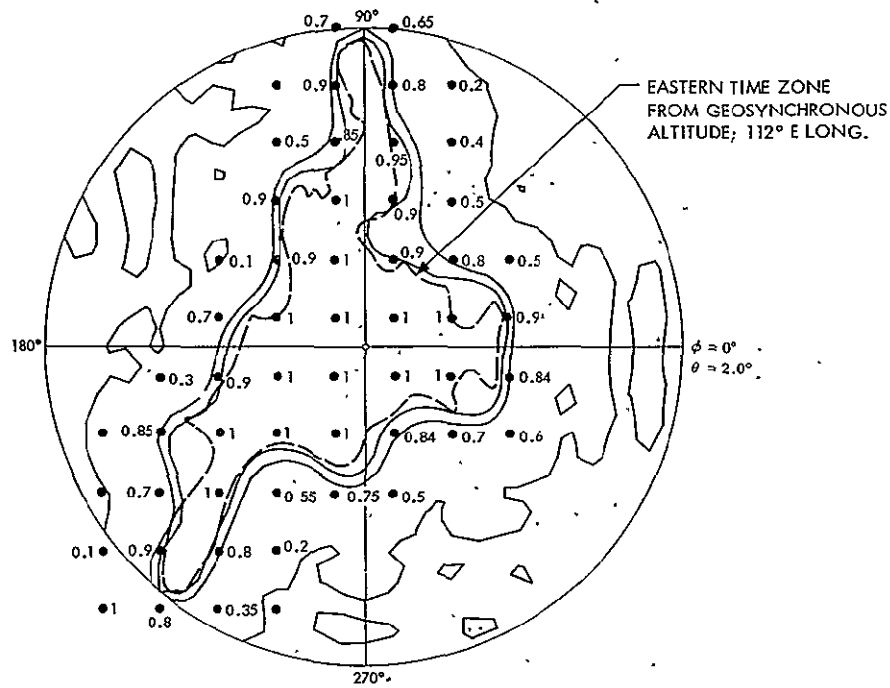
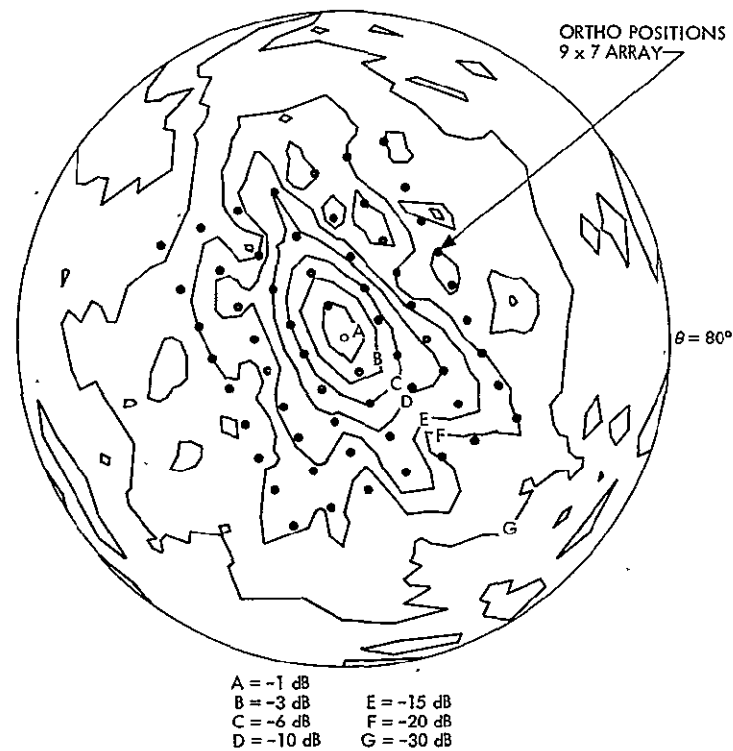Figure A-6. Orthogonal Beam Summation, Eastern Time Zone Contour Fit

A = -1 dB
B = -3 dB   E = -15 dB
C = -6 dB   F = -20 dB
D = -10 dB   G = -30 dB

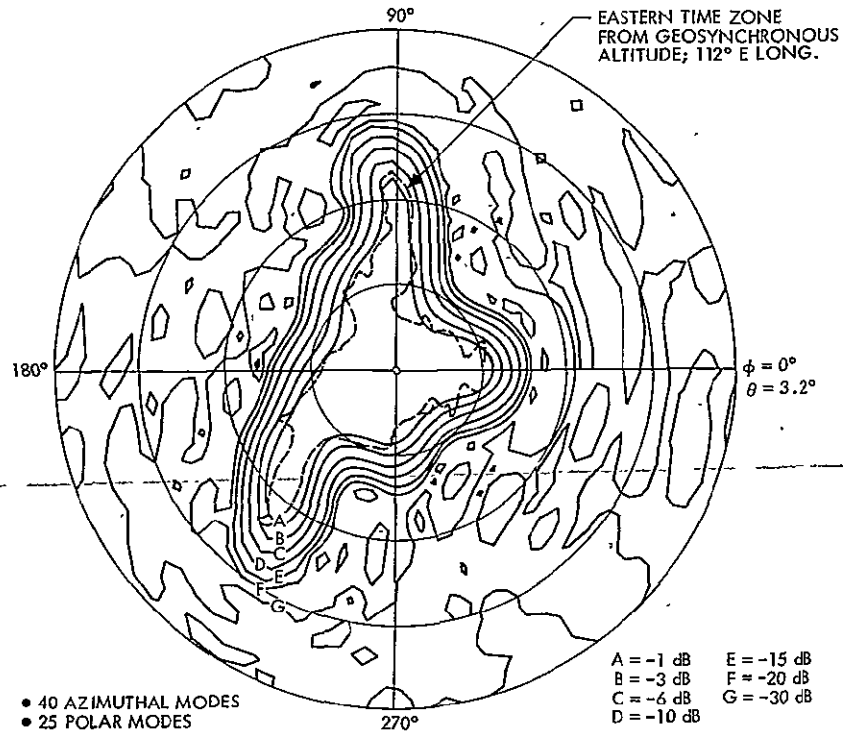Figure A-7. Required Feed Pattern, Eastern Time Zone Contour Fit

Figure A-8. Final Secondary Pattern,
Eastern Time Zone Contour Fit

3.   SUMMARY

Developments in the broad general area of scanning technology
(which can be extended to include multiple-beam and contoured beam
antennas) are expected to be rapidly applied to a number of current
antenna system problems.

APPENDIX B

COMPARISON OF SPHERICAL AND

PARABOLOID REFLECTOR

SCAN CAPABILITIES

The question often arises as to whether spherical reflectors are a better choice than paraboloid reflectors for beam scanning or multiple-beam applications and, if so, under what conditions. To answer this question, calculations were made to determine, for a given antenna size and f/D, how far the beam of a paraboloid could be scanned before the scan loss associated with the paraboloid was equal to the aberration loss of a sphere with the same aperture size and f/D. In each case, a simple point-source feed, in contrast to aberration-compensating feeds, was assumed. This is a reasonable assumption in that if an aberration-correcting feed is used with a spherical reflector, then it is reasonable to allow the use of compensated feeds or shaped reflector techniques to improve the scanning performance of a paraboloid. If aberration or scan-compensated feeds are used, the comparison becomes more complex and very likely would not give a great deal more insight into the problem, at least not within the accuracies of the assumptions used in these calculations.

The comparisons were made assuming that each antenna had uniform illumination across its aperture since loss data and effective f/D ratios are available only for the spherical reflectors (Refs. B-1, B-2, B-3). The scan properties for a paraboloid were obtained from a general curve developed by Ruze (see Ref. A-1). This scan data is good only to the accuracy that the data can be read from the curves and the degree that the universality of the curve applies to large f/D ratios. It should be pointed out that Ruze developed his data using small-angle approximations. These approximations limit his data to very large diameters when large f/D ratios and scan angles must be used. As an example, for 10 beamwidths of scan (in terms of 3-dB beamwidth at bore-sight) and f/D = 1.0, the reflector diameter should be on the order of 800 wavelengths or larger to meet the small-angle criterion. At this time, data is not available to indicate the magnitude of the errors that might exist if this criterion is not met. Thus, some discretion must be used when interpreting data plotted in Figs. B-1 and B-5 for large scan angles or large f/D ratios. Also, to simplify the tradeoff analysis, feed blockage was not considered.

In this report, large reflectors are of primary interest. For paraboloids with f/D ratios of 1.5 or less and with diameters of 200 wavelengths or greater, the blockage losses are less than 0.3 dB. The assumption was also made that blockage would be similar for both reflector types under similar conditions. Thus, ignoring blockage in the comparison appears to be reasonable. Finally, it was found that small errors in reading the loss data for small scan angles caused large variations in the conclusions associated with paraboloid reflectors with large f/D ratios. For the above reasons, the data obtained is considered usable primarily for making comparisons between the two reflector types and is not recommended for design purposes.

Figure B-1 displays the scan angle, in beamwidths of scan, at which the scan loss of a paraboloid reflector has increased to equal the aberration loss of a spherical reflector. It is interesting to note that, for the smaller f/D ratios, paraboloids can be scanned over a large number of beamwidths before a sphere can be used advantageously.
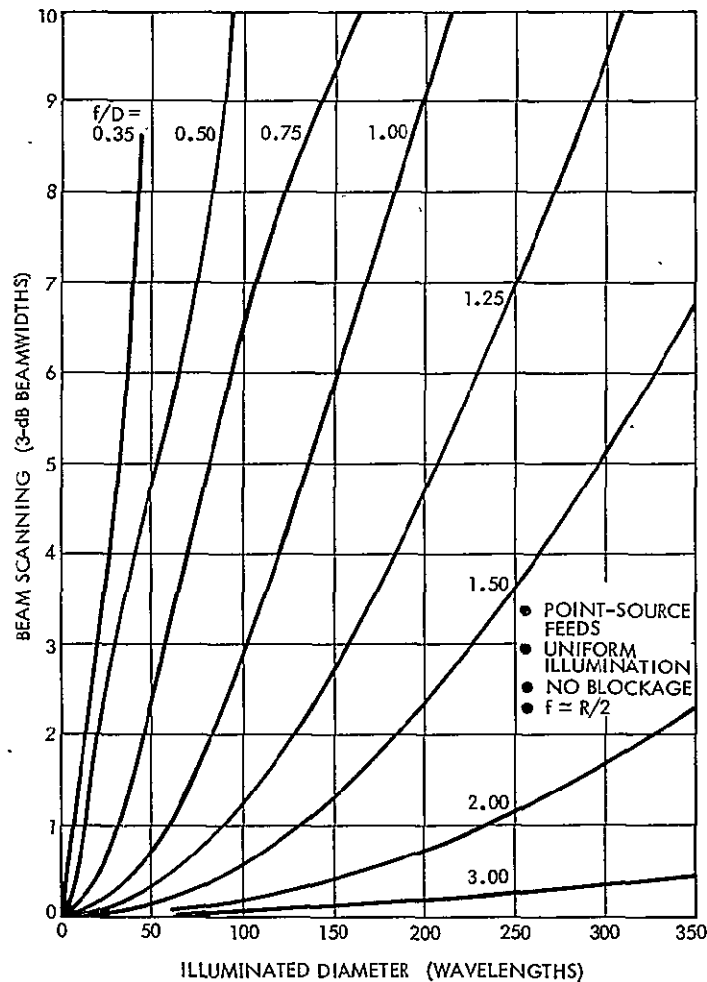
Figure B-1. Beam Scan at Which Scan Loss
of a Paraboloid Equals Aberration
Loss of a Sphere

Figure B-2 shows the aberration losses associated with spherical reflectors, assuming no aperture blockage. It should be pointed out that the spherical reflector aberration loss is essentially independent of scan angle. The diameter of a spherical reflector must be increased over that needed for the illuminated aperture if there is a requirement to support multiple beams or beam scanning. Figure B-3 illustrates how much larger the spherical reflector must be for a given scan angle and various f/D ratios. The lower right boundary to the curves is limited by the case in which the spherical reflector subtends a half-angle of 90 deg relative to the center of the sphere; therefore, at the lower boundary, the focal region extends from the focal point (approximately half-way between the spherical reflector and the center of the sphere) to the reflector surface.
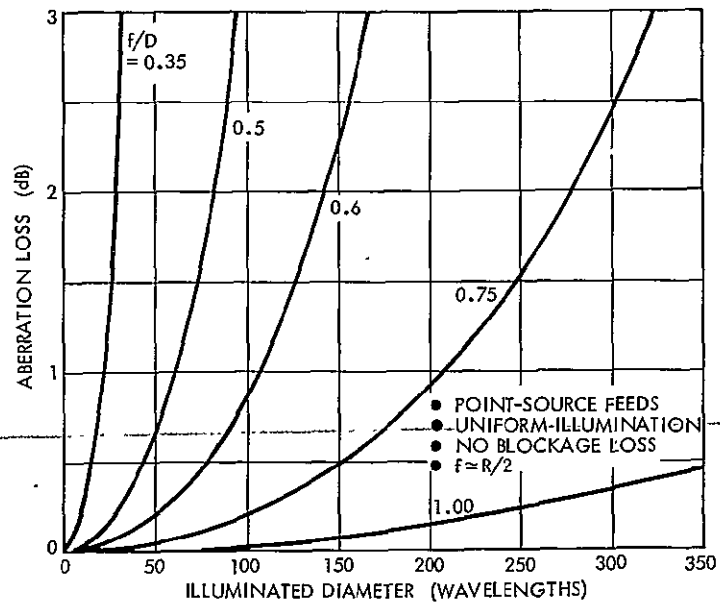
Figure B-2.   Spherical Reflector
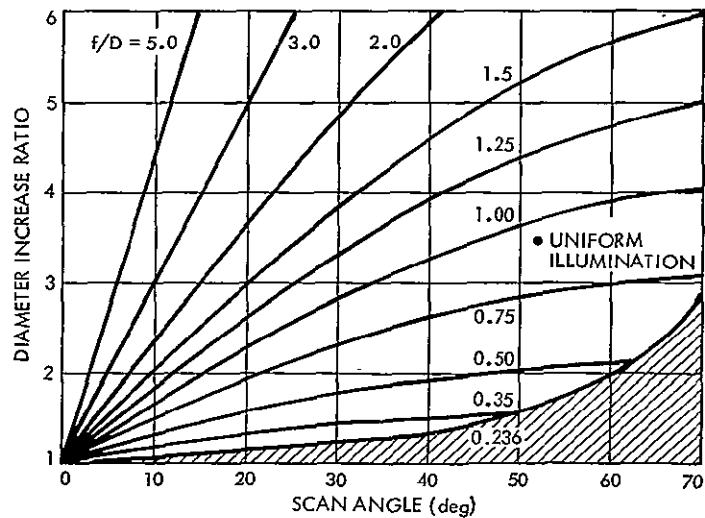Aberration Loss

Figure B-3.   Spherical Reflector
Diameter Increase With
Scan Angle

Figure B-4 is included only to show how long a line-source feed would be required if aberration correction for a spherical reflector were desired. It should be noted that the smaller the f/D ratio, the longer the feed must be, with the length requirement accelerating for f/D values less than 1.0. For f/D of approximately 0.25, a line-source feed reaching from the focal point to the reflector is required.

Generally, the primary advantage of aberration correcting is to allow the use of smaller f/D ratios, which in turn results in reducing the reflector size increase required to support a given scan requirement. However, in deciding whether to use a line-source feed or not, several factors should be considered. It is difficult to design multiple-frequency line-source feeds for antenna systems requiring coincident beams at several frequencies or frequency bands. Also, larger reflectors with small f/D ratios imply long line-source feeds. Long line-source feeds, however, can suffer from excessive dissipation losses and very narrow bandwidths. If small f/D ratios are necessary to reduce reflector costs and aberration losses must be kept small, aberration-correcting array feeds and/or secondary reflectors might also be considered instead of line-source feeds.

Figure B-5 shows typical scan losses for paraboloids, assuming no blockage and uniform aperture distributions. It should be pointed out that the scan loss is essentially independent of antenna size. Figure B-6 shows the loss corrections that must be made for paraboloids to account for aperture blockage, if it is assumed that the area covered by the scanning feed constitutes aperture blockage. Since strut blockage and diffraction effects were not included and uniform illumination was assumed, the blockage loss could be larger. Figures B-2 and B-5 can then be used to compare the losses of the two reflector types if one remembers that the spherical reflector performance does not change appreciably with scan angle and the paraboloid loss does not change appreciably with diameter. Although data has been included for blockage of a sphere and paraboloid, as was noted earlier, blockage effects were not included in the comparisons between the reflectors.

Going back to Fig. B-1, for a given reflector size and f/D, as scan requirements increase, the paraboloid reflector scan loss goes up while the spherical reflector loss remains constant. Therefore, for scanning beyond the crossover scan angle, spherical reflectors are more advantageous; for less than this angle, paraboloids are more advantageous. Also, for a given scan requirement and f/D, as the reflector size increases, the paraboloid scan loss remains essentially constant while the spherical reflector aberration loss increases. Therefore, as the diameter increases from the crossover case, paraboloids are more desirable; and for smaller diameters, spherical reflectors are more desirable. An important point to consider is that for the larger f/D ratios, the scan loss or aberration loss (Fig. B-2) varies slowly with changes in f/D. Therefore, in this region, the crossover scan angle should be considered to be quite broad and the choice of paraboloid vs. sphere should be based on other considerations.
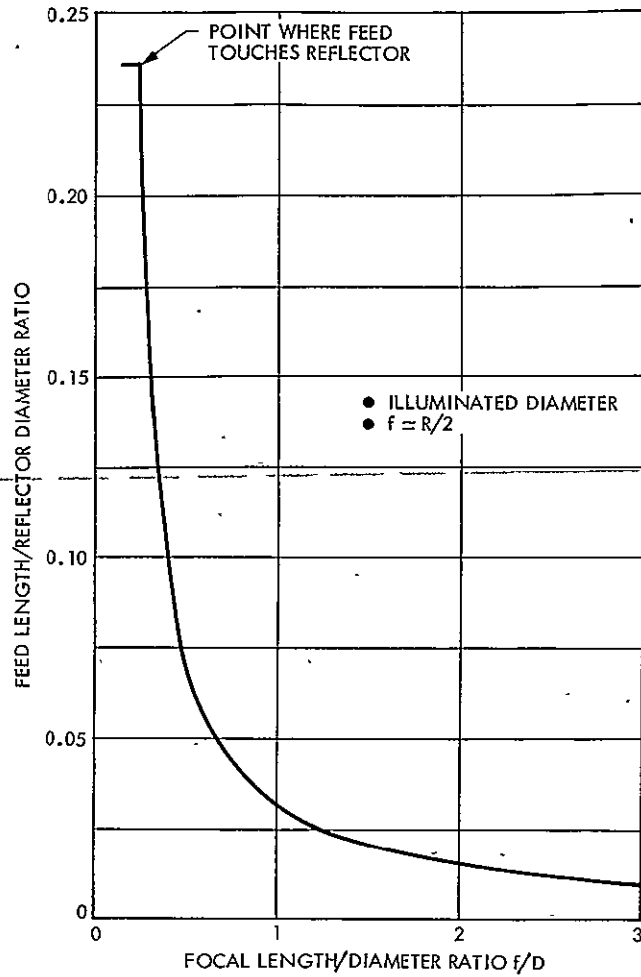
Figure B-4. Spherical Reflector Axial
Focal Region Length

The temptation to go to f/D values in excess of 1.0 to reduce aberration or scan loss must be weighed against the cost of building longer focal-length antennas and, for the spherical reflector, the necessity to increase the size of the reflector diameter for a given scan angle as the f/D ratio gets larger. Figure B-2 shows that, for f/D ratios greater than 1.0, the improvements in aberration loss are on the order of a few tenths of a decibel; these improvements must be weighed against the increased system costs.

The following is an example of a typical tradeoff, where blockage is not considered. In Fig. B-1, a spherical reflector and a paraboloid with f/D = 1.0 and diameter of 217 wavelengths have the same performance at a scan angle of 10 beamwidths. Now, the following expression relates the scan angle N_B, in beamwidths, to the scan angle N_D, in degrees, for
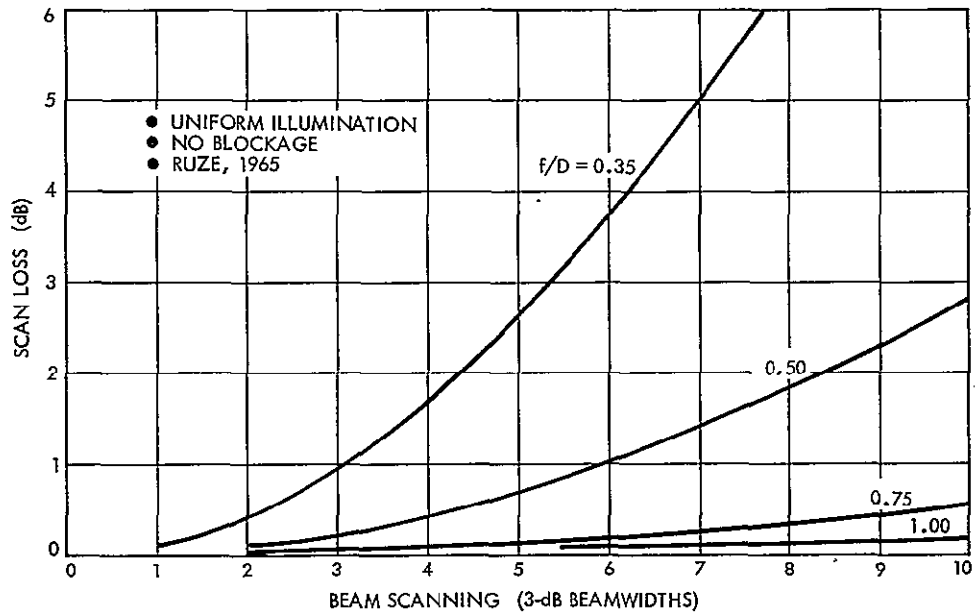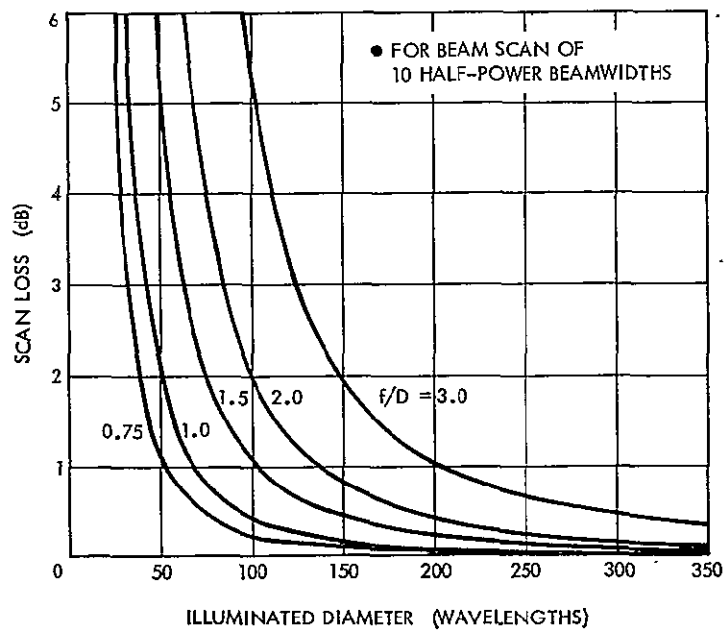
Figure B-5. Paraboloid Scan Loss

Figure B-6. Paraboloid Scan Loss
Due to Aperture Blockage

a given antenna diameter in wavelengths with a uniformly illuminated aperture:

$$N_D = 58.4 \frac{\lambda}{D} N_B$$

where D is the antenna diameter and λ is the wavelength. In Fig. B-3, then, a spherical reflector 1.2 times the illuminated aperture diameter is required to get 10 beamwidths of scan (2.7-deg scan angle). If the f/D is increased to 2.0, the spherical reflector diameter must now be 1.4 times the effective aperture diameter, and for f/D = 5.0, 2.0 times. Thus, increasing f/D to improve scan performance can be costly in antenna size, especially where the improvement may not be significant (on the order of 0.1 dB). From Fig. B-2, it may be seen that for diameters less than 350 wavelengths and f/D greater than 1.0, the losses are less than 0.5 dB. However (from Fig. B-1), for this loss (and associated illuminated aperture size of 350 λ), paraboloids with f/D = 1.0 can scan in excess of 10 beamwidths. So, for moderate scan requirements, paraboloid reflectors are usable, are smaller in diameter, and have the advantage of a wider variety of applications.

Table B-1 illustrates the use of a spherical reflector at earth synchronous altitude for ±7.5 deg coverage (scan angle at which large, uncompensated-fed paraboloids would not be usable). The parameters were selected to give the minimum total efficiency loss resulting from reflector aberration loss and the blockage loss caused by the feed system. All the calculations are again based on the assumption of uniform aperture illumination. Several conclusions can be drawn from Table B-1. First, as the illuminated aperture size is increased, the f/D must be enlarged to minimize the losses. Second, the minimum loss increases with illuminated aperture size. Third, the reflector overall diameter must be larger than the illuminated diameter to support the beams which are directed away from the antenna axis. As the illuminated diameter is increased, for the same angular coverage of ±7.5 deg, the overall diameter must be increased by a larger amount. For example, for a 100-λ aperture, the size must be increased by 40% to 140 λ. However, for a 1000-λ aperture, the size must be increased by 73% to 1730 λ. It should be pointed out that the blockage loss shown in Table B-1 applies to the central beams. For the beams pointed away from the antenna axis, the blockage loss becomes less as the projected feed cluster area moves out of the illuminated portion of the spherical reflector associated with the scanned beam. Table B-1 also lists the number of 10-dB-beamwidth spaced individual beams that can be supported by each antenna size and the corresponding earth footprint if the antenna is assumed to be at synchronous altitude.

Table B-1. Typical Properties of Multiple-Beam Spherical Reflector[a]

Illuminated Aperture Diameter, Wavelengths	f/D	Loss, dB			Required Increase in Reflector Diameter, %	Available Beams		10-dB Beamwidth Earth Footprint at Nadir, km
		Aberration	Blockage	Total		One Direction	Total	
50	0.66	0.12	0.39	0.51	32	8	58	1243
100	0.79	0.14	0.49	0.63	40	16	206	621
200	0.95	0.20	0.64	0.84	48	31	769	311
350	1.10	0.26	0.82	1.08	56	53	2286	178
500	1.20	0.31	0.97	1.28	61	76	4609	124
700	1.31	0.38	1.14	1.52	67	106	8959	89
1000	1.43	0.46	1.36	1.82	73	152	18170	62

[a]Angular coverage = ±7.5 deg (typical earth synchronous altitude application). Assumptions: uniform illumination, beams spaced 10-dB beamwidths apart.

The following conclusions were drawn from the study:

(1)   For modest scan requirements (of the order of 10 beamwidths), paraboloids with f/D of the order of 1.0 or greater appear to be more advantageous than spherical reflectors, for illuminated diameters of 200 λ or larger.

(2)   For scan requirements much greater than 10 beamwidths, spherical reflectors have an advantage, with the advantages increasing as the scan requirements increase for large reflector applications. A disadvantage is the need to increase the reflector diameter beyond that required for the illuminated aperture area, which is a function of the scan requirement.

(3)   At the point where the paraboloid and the spherical reflector have the same performance, increasing the scan requirement favors the spherical reflector, while decreasing scan favors the paraboloid. Also, increasing the reflector size favors the paraboloid, while decreasing size favors the spherical reflector. However, for large f/D and diameters, the tradeoff region is quite broad.

(4)   A more extensive study is required to determine the accuracy and/or the correctness of the above conclusions under practical conditions such as using realizable illumination functions and blockage and eliminating the assumptions and interpolation errors that are inherent in the data used for performing the scan and aberration loss tradeoffs.